Available online at www.CivileJournal.org

Civil Engineering Journal

(E-ISSN: 2476-3055; ISSN: 2676-6957)

Vol. 12, No. 05, May, 2026

Impact of Cooling Methods on the Valorisation of Calcined Dam Sediments in Self-Compacting Concrete

Ahmed Sweiti [1*], Rabah Chaid [2], El-Hadj Kadri [3]

[1] *Civil Engineering, Mechanical Solids and Systems Laboratory, University M'hamed Bougara of Boumerdes, Cite Frantz Fanon 35000, Algeria.*

[2] *Civil Engineering, Research Unit: Materials, Processes and Environment (UR-MPE), University M'hamed Bougara of Boumerdes, Cite Frantz Fanon 35000, Algeria.*

[3] *Mechanics and Civil Engineering Materials Laboratory (L2MGC), University of CY-Paris, Cergy-Pontoise 95031, France.*

Received 07 February 2026; Revised 19 April 2026; Accepted 22 April 2026; Published 01 May 2026

Abstract

Dam sedimentation poses critical environmental and operational challenges worldwide, requiring sustainable valorisation strategies. This study investigates how post-calcination cooling protocols influence the pozzolanic performance of Ksob dam sediments (Algeria) as a partial cement replacement in self-compacting concrete (SCC). Raw sediments were calcined at 750 °C for 5 h and subjected to three cooling methods: water quenching (WQCS), air cooling (ACCS), and slow furnace cooling (SCCS). Ten SCC formulations were prepared with 10%, 15%, and 20% cement substitution rates. Despite the reduced binder content, all mixtures maintained self-compacting properties (spread: 700-735 mm; T_{500}: 1.06-1.39 s) with moderate superplasticiser adjustment, up to 1.2% of binder mass. WQCS formulations exhibited superior performance: at 10% substitution, compressive strength reached 97% of the control at 180 days, while water absorption and permeable porosity decreased relative to the control by 7.1% and 1.9%, respectively. TGA/DSC analysis attributed these gains to enhanced pozzolanic C-S-H formation. These findings demonstrate that cooling kinetics critically govern the mineralogical transformation and reactivity of calcined sediments. Water quenching proved optimal for producing high-performance, eco-efficient SCC, offering a viable pathway for large-scale dam sediment valorisation while lowering the cement industry's carbon footprint.

Keywords: Dam Sediments; Thermal Activation; Self-Compacting Concrete; Pozzolanic Reactivity; Sustainable Construction.

1. Introduction

Dam sedimentation represents one of the most pressing environmental and operational challenges facing water resource management globally. Every year, an estimated 1% to 2% of total reservoir storage capacity is lost worldwide due to sediment accumulation [1], reducing water availability, increasing flood risk downstream, and shortening the operational lifespan of hydraulic infrastructure [2]. In Algeria alone, more than 50 major dams are facing accelerated silting rates, threatening both agricultural irrigation and drinking water supply. Conventional management strategies, primarily dredging followed by landfill disposal [3], are increasingly recognised as economically unsustainable and ecologically damaging, generating secondary contamination risks and consuming significant land resources.

In this context, the valorisation of dredged dam sediments within the construction materials sector has emerged as a scientifically credible and economically attractive alternative, fully aligned with circular economy principles [4-7].

* Corresponding author: a.sweiti@univ-boumerdes.dz

https://doi.org/10.28991/CEJ-2026-012-05-03

Rather than treating sediments as waste, this approach transforms them into value-added resources, contributing to the reduction of natural raw material extraction, waste generation, and industrial CO_2 emissions [8-10]. The production of ordinary Portland cement (OPC) alone accounts for approximately 8% of global CO_2 emissions, making partial cement substitution with supplementary cementitious materials (SCMs) a critical lever for decarbonising the construction sector [11].

The thermal activation of dam sediments, primarily composed of kaolinitic clay minerals, is central to their use as pozzolanic SCMs [12-15]. At temperatures between 600 °C and 900 °C, kaolinite undergoes dehydroxylation ($Al_2Si_2O_5(OH)_4 \rightarrow Al_2Si_2O_7 + 2H_2O$), yielding amorphous metakaolinite. This disordered phase exhibits high pozzolanic reactivity, reacting with portlandite ($Ca(OH)_2$), a by-product of cement hydration, to form secondary calcium silicate hydrates (C-S-H) and calcium aluminosilicate hydrates (C-A-S-H), thereby densifying the cement paste microstructure and enhancing mechanical and durability performance. Critically, the degree of amorphisation achieved during thermal treatment, and thus the ultimate pozzolanic reactivity of the calcined product, is not solely governed by calcination temperature and dwell time, but is also strongly influenced by the kinetics of post-calcination cooling. Rapid quenching has been shown to preserve the disordered metastable state by preventing recrystallisation, while slow cooling may allow partial structural reorganisation, reducing reactivity. Despite its acknowledged importance in ceramic and geopolymer science, this cooling-kinetics variable has received little systematic attention in the context of dam sediment valorisation.

Several studies have confirmed the feasibility of incorporating calcined dam sediments as partial cement replacements in conventional vibrated concrete [16-20], reporting improvements in long-term mechanical strength, reduced permeability, and enhanced durability attributable to secondary pozzolanic C-S-H formation. Safer et al. [19] demonstrated that calcined sediments from Chorfa dam (Algeria) could replace up to 30% of cement in conventional concrete without compromising compressive strength at 90 days, while Rozière et al. [21] confirmed durability improvements for dredged marine sediment-based concrete at 20% substitution. However, incorporating calcined sediments into self-compacting concrete (SCC) presents a substantially more demanding challenge. SCC, first developed in Japan in the late 1980s [22], achieves compaction under its own weight without mechanical vibration [23], requiring the simultaneous satisfaction of three stringent rheological criteria: adequate flowability (filling capacity), sufficient viscosity (resistance to dynamic segregation), and passability ability through confined reinforcement. These properties are highly sensitive to the physical characteristics of SCMs, including specific surface area, particle morphology, and surface chemistry, making the integration of calcined sediments into SCC formulations considerably more complex than in ordinary concrete.

To date, only a limited number of studies have investigated the incorporation of calcined sediments into SCC [21, 24-27]. These works have established the general feasibility of the approach and confirmed that calcined sediments can contribute to SCC performance, particularly at substitution rates of 10-20%. Nevertheless, a critical and unresolved gap persists in the literature: no study has systematically investigated the effect of the post-calcination cooling method on the mineralogical structure, pozzolanic reactivity, and resulting SCC performance of dam sediments. This knowledge gap is particularly significant because, as demonstrated in calcined clay and metakaolin research [12-15], cooling kinetics directly control the degree of amorphisation of the thermally treated material and, therefore, its capacity to participate in secondary hydration reactions over time. Whether water quenching, air cooling, or slow furnace cooling produces meaningfully different outcomes in the context of full-scale SCC formulation across fresh-state rheology, long-term mechanical strength, and durability remains entirely uncharacterised.

The present study addresses this gap through a systematic experimental investigation of Ksob dam sediments (Wilaya of M'Sila, Algeria), calcined at 750 °C for 5 hours and subjected to three post-calcination cooling protocols: water quenching (WQCS), air cooling (ACCS), and slow furnace cooling (SCCS). Ten SCC formulations were developed with cement substitution rates of 10%, 15%, and 20% by mass. The study pursues three principal objectives: (i) to quantify the influence of the cooling method on the mineralogical and morphological characteristics of calcined sediments using XRD and TGA/DSC analyses; (ii) to evaluate the impact of these sediments on the fresh-state rheological, hardened-state mechanical, and long-term durability properties of SCC; and (iii) to establish mechanistic correlations between cooling mode, cement paste microstructure, and macroscopic concrete performance, thereby providing a scientific basis for the optimisation of dam sediment calcination protocols for use in eco-efficient SCC production.

Although previous research has established the feasibility of incorporating calcined dam sediments into SCC, a critical limitation remains: existing studies completely overlook the thermodynamic trajectory of the material post-calcination. Specifically, the influence of cooling kinetics—which dictate the preservation of the highly reactive, amorphous metakaolinite phase—has never been systematically investigated in the context of SCC. This work uniquely addresses this gap by isolating the cooling method (water, air, and slow cooling) as a primary variable, and demonstrating how these cooling-induced mineralogical variations directly govern the fresh-state rheology, pozzolanic reactivity, mechanical properties, and long-term durability of SCC.

2. Experimental methodology

2.1. Materials

- ***Cement*:** Portland cement type CEM I 42.5, complying with standard NF EN 197-1 [28], from the GICA cement plant in Ain El Kebira (Algeria) was used. This cement had a clinker content of at least 95%, a Blaine Specific Area of 3129 cm^2/g and a density of 3.1 g/cm^3.
- ***Sediments*:** Sediments were taken from the Ksob dam reservoir (Wilaya of M'Sila, Algeria).
- ***Aggregates*:** Limestone aggregates (0/3 sand, 3/8 and 8/15 gravel) from the Bouzegza Quarry (Boumerdes, Algeria) were used. Dune sand (0/2) from Oued Souf was added to correct the granulometry [29].
- ***Admixtures*:** A superplasticiser/high water reducer of the Sika ViscoCrete 4050 RMX type (density 1.1 ± 0.015, dry extract 70%) was used [30].

2.2. Preparation and Characterisation of Calcined Sediments

The raw sediments were collected during a dredging operation, first air-dried and subsequently oven-dried at 105 °C for 24 hours to remove residual moisture. After drying, the sediments were ground in a ball mill and sieved through an 80 µm mesh to obtain a fine, homogeneous powder of uncalcined sediment (**US**) with a Blaine Specific Area of approximately 13,000 cm^2/g. Fine grinding was intended to increase the reactivity of the sediments and the compactness of the resulting concrete mixtures [31].

The calcination temperature of 750 °C was selected based on the dehydroxylation range of kaolinite (550-900 °C) identified by TGA/DSC analysis of raw sediments, consistent with the literature [12-15]. The theoretical basis for the influence of cooling kinetics on pozzolanic reactivity lies in the thermodynamic stability of the amorphous metakaolinite phase. During calcination, the dehydroxylation reaction $Al_2Si_2O_5(OH)_4 \rightarrow Al_2Si_2O_7 + 2H_2O$ produces a highly disordered, metastable aluminosilicate phase. The 5-hour dwell time was chosen to ensure uniform heat penetration and complete phase transformation of kaolinite to amorphous metakaolinite without inducing mullitisation or excessive sintering above 900 °C, which would reduce pozzolanic reactivity. A heating rate of 10 °C/min was applied, as is standard for laboratory-scale calcination.

Three cooling methods were applied:

1. **Water quenching (WQCS)**: Rapid cooling by immersion in water immediately after calcination.
2. **Air cooling (ACCS):** Cooling to room temperature in the open air immediately after calcination.
3. **Slow cooling (SCCS):** Gradual cooling in the furnace for 24 hours.

A sample of the **uncalcined sediment (US)** was retained as a reference. The four products (**US**, **WQCS**, **ACCS, SCCS**) were packaged in sealed plastic bags.

Table 1 shows the chemical composition of the different sediments and cement used

Table 1. Chemical compositions of cement and sediments (calcined and raw) in %

Constituents	Cement	WQCS	ACCS	SCCS
SiO_2	21.12	44.97	44.34	42.99
Al_2O_3	4.51	15.58	12.83	14.51
Fe_2O_3	4.66	5.72	4.97	5.40
CaO	64.70	21.09	23.83	21.07
MgO	1.33	2.11	1.98	1.99
SO_3	2.13	0.16	0.17	0.15
K_2O	0.32	1.90	1.57	1.78
Na_2O	0.11	0.46	0.41	0.41
P_2O_5	NA	0.28	0.26	0.30
TiO_2	NA	0.83	0.73	0.80
Loss on ignition	0.74	6.9	8.92	10.61

The overall experimental procedure is summarised in Figure 1.

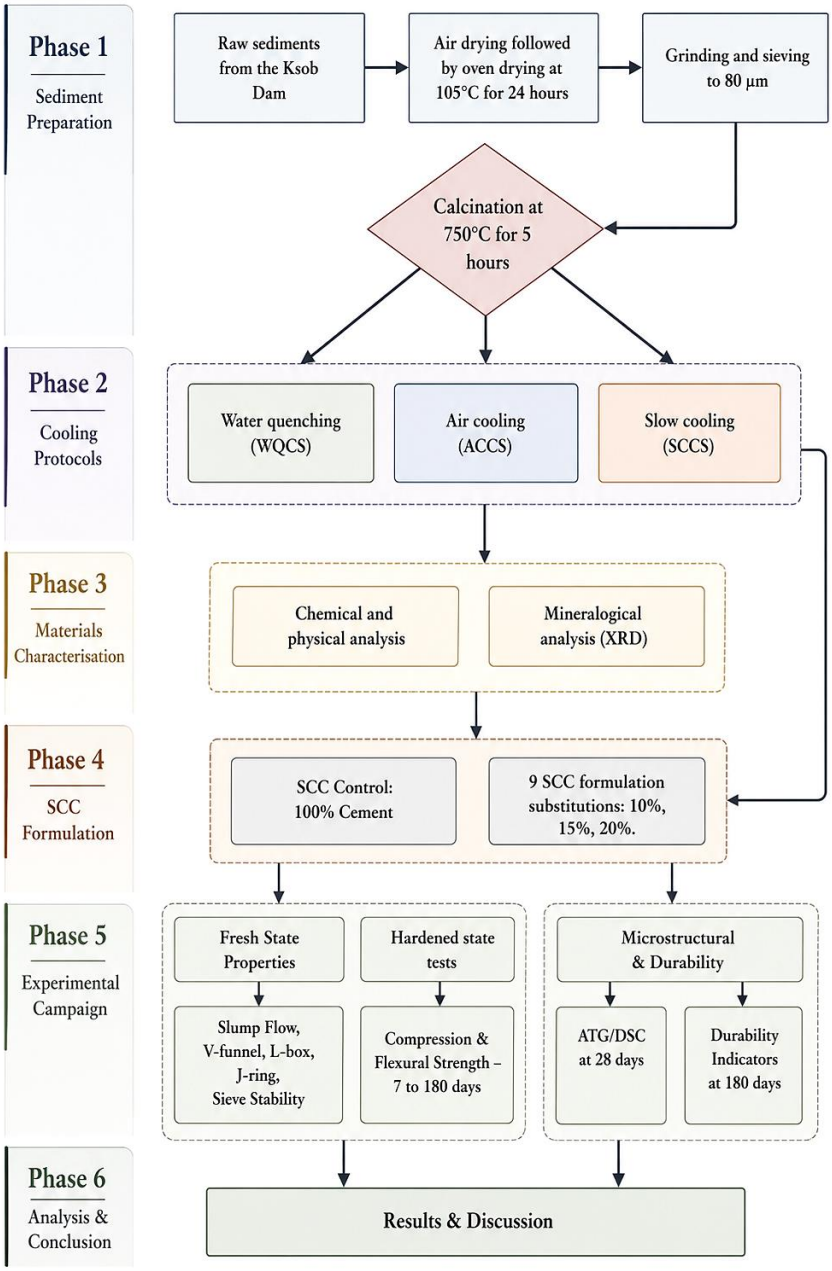

Figure 1. The flowchart of experimental procedure

Table 2 presents the physical and chemical characteristics of the cement used, determined in accordance with European standards:

Table 2. Physicochemical properties of cement used

Characteristics	Standard	Average
Loss on ignition (%)	0.740	
Insoluble residue (%)	0.45	
Magnesium oxide content (%)	1.33	NF EN 196-2 [32]
Sulphuric anhydrite content (%)	2.13	
Chloride (%)	< 0.010	
Blaine fineness (cm^2/g)	3129	NF EN 196-6 [33]
Setting time (min)	190	NF EN 196-1 [34]
Expansion (Le Chatelier) (mm)	0.0	

The mineralogical composition of cement, determined by X-ray diffraction (XRD), is shown in Table 3.

Table 3. Mineralogical composition of cement

Phase	Mineral constituents of clinker	Content relative to clinker (%)
Clinker	C_3S	56
	C_2S	22
	C_3A	04
	C_4AF	15
	Free CaO	< 02
Setting regulator	Gypsum	04
Addition	No addition	No addition

The mechanical strength of cement, measured on standardised mortars in accordance with NF EN 196-1, is shown in Table 4.

Table 4. Results of mechanical tests on cement

Age in days	Flexural strength (N/mm²)	Compressive strength (N/mm²)
02 days	4.2	19.4
28 days	7.7	48.1

The particle size analysis was carried out in accordance with standard NF EN 933-1 [35], enabling the particle size curves to be plotted and the fineness modulus of the two sands to be calculated. Table 5 summarises the particle size analysis results for the four fractions used.

Table 5. Results of particle size analysis

Fraction	Fineness modulus	Maximum diameter (mm)	Classification	Regulatory compliance
Dune sand (0/2)	1.98	2.5	Fine	Correction required
Quarry sand (0/3)	3.44	3.15	Coarse	Correction required
Gravel (3/8)	-	8	Fine gravel	Compliant
Gravel (8/15)	-	16.0	Medium gravel	Compliant

The particle size distribution curves of the four fractions are illustrated in Figure 2, confirming the combined use of dune and quarry sands to correct the overall grading.

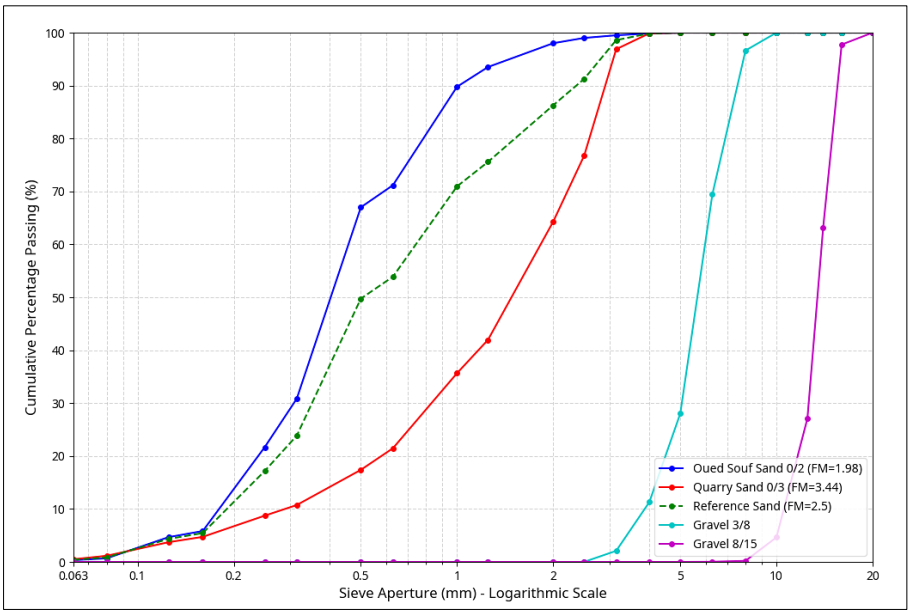

Figure 2. Aggregate particle size distribution curves

X-ray diffraction (XRD) mineralogical analysis was performed on the four sediment samples to identify the crystalline phases and evaluate the effect of calcination and cooling on the pozzolanic activity of the sediments.

The X-ray diffractogram of the uncalcined sediment shows well-defined and intense crystalline peaks, characteristic of a highly crystalline material. The main minerals identified are: Kaolinite, Quartz, Calcite, and Illite. This mineralogical signature reflects the natural composition of the sediments prior to any thermal treatment.

After calcination at 750 °C, the three cooling methods distinctly alter the crystalline signatures observed. It can be seen that the kaolinite peaks initially present in the spectrum of the uncalcined sediment (US) (Figure 3), gradually diminish depending on the cooling method: they remain faintly visible after slow cooling (SCCS) (Figure 4), fade further during air cooling (ACCS) (Figure 5) and disappear almost entirely after water quenching (WQCS) (Figure 6).

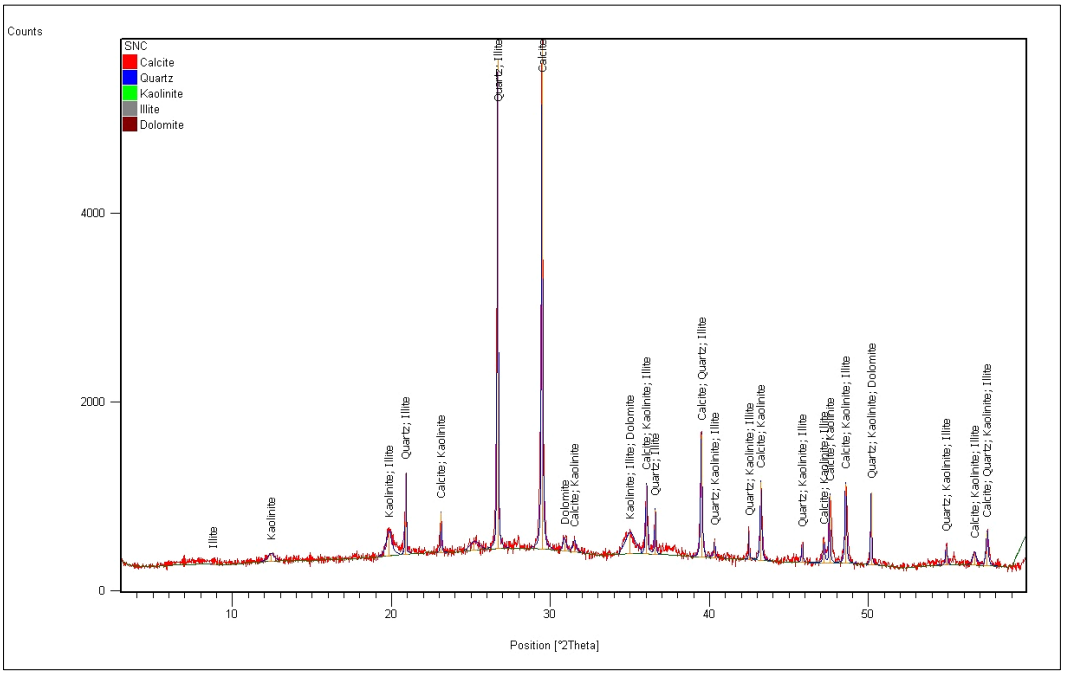

Figure 3. XRD pattern of US

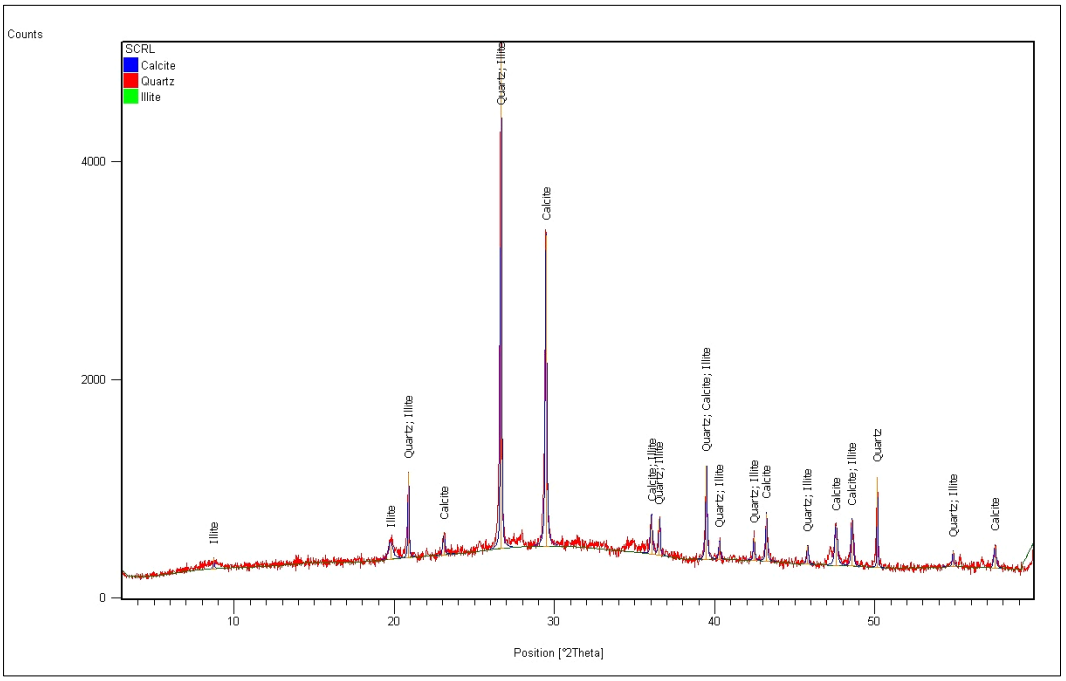

Figure 4. XRD pattern of SCCS

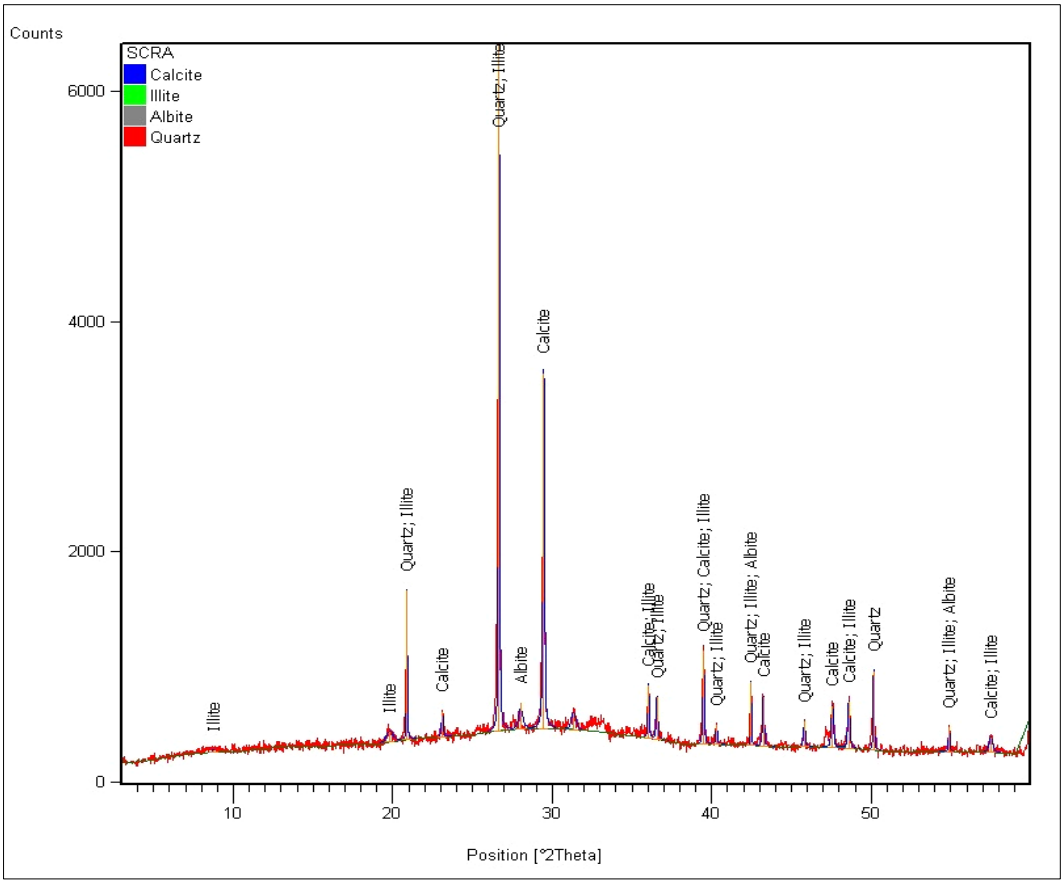

Figure 5. XRD pattern of ACCS

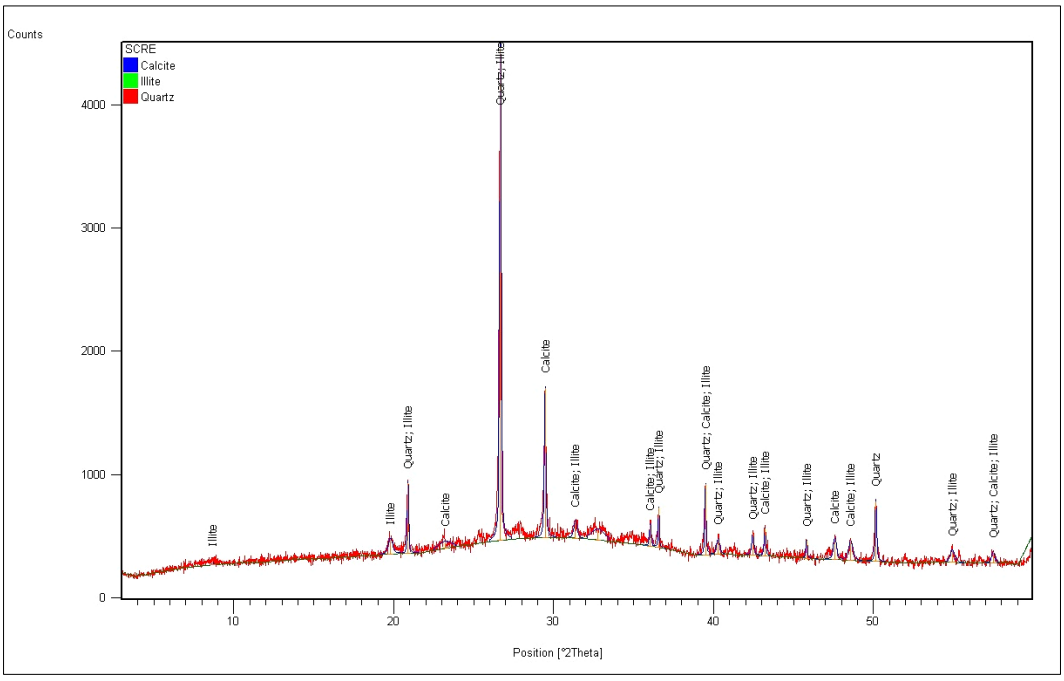

Figure 6. XRD pattern of WQCS

2.3. Formulation and Preparation of Self-Compacting Concrete (SCC)

Ten SCC formulations were studied [36]: a control formulation (CTR) with 100% cement, and nine formulations in which the cement was replaced by 10%, 15% or 20% (by mass) of calcined sediments (WQCS, ACCS and SCCS). The water and superplasticiser were adjusted to maintain a targeted self-compacting consistency, taking into account the higher water demand of the sediments (confirmed by a preliminary Vicat test). The detailed compositions are shown in Table 6.

Table 6. Composition of SCCs (kg/m³)

Constituents	CTR	S10	A10	W10	S15	A15	W15	S20	A20	W20
Cement CEM I 42.5	450	405	405	405	382.5	382.5	382.5	360	360	360
SCCS	0	45	0	0	67.5	0	0	90	0	0
ACCS	0	0	45	0	0	67.5	0	0	90	0
WQCS	0	0	0	45	0	0	67.5	0	0	90
Total binder	450	450	450	450	450	450	450	450	450	450
Water	184.5	189	189	189	189	189	189	193.5	193.5	193.5
Superplasticiser	4.95	4.95	4.95	4.95	5.40	5.40	5.40	5.40	5.40	5.40
Dune sand (0/2)	529	529	529	529	529	529	529	529	529	529
Quarry sand (0/3)	311	311	311	311	311	311	311	311	311	311
Gravel (3/8)	360	360	360	360	360	360	360	360	360	360
Gravel (8/15)	539	539	539	539	539	539	539	539	539	539
W/B Ratio	0.41	0.42	0.42	0.42	0.42	0.42	0.42	0.43	0.43	0.43
SP (% Binder)	1.10	1.10	1.10	1.10	1.20	1.20	1.20	1.20	1.20	1.20

2.4. Test Methods

- **Fresh state:** The SCC was characterised in its fresh state: spread on the Abrams cone, flow through the V-funnel, filling capacity in the L-box, stability on the sieve, flow through the J-ring in accordance with the recommendations, as well as measurement of density and air content using pressure methods.
- **Hardened state (mechanical properties):** Prismatic test specimens (10 × 10 × 40 cm^3) were prepared for each formulation and stored in water at 20 ± 1 °C. Compressive and flexural strength tests were performed at 7, 14, 28, 90 and 180 days.
- **Thermal Analysis (TGA/DSC):** Thermogravimetric analysis (TGA) and differential scanning calorimetry (DSC) were performed at a heating rate of 10 °C/min to evaluate portlandite consumption and hydrate formation in cement pastes (controlled and with 10% and 15% ACCS and WQCS, respectively) prepared and hydrated for 28 days, then dried at 80 °C and ground.
- **Durability:** Prismatic test specimens (7 × 7 × 28 cm^3) were stored in water for 180 days. Durability indicators (water absorption by immersion and boiling, permeable pore space and densities) were determined according to ASTM C642-13 [37].

3. Results

3.1. Fresh properties

The fresh properties of the different SCC formulations are presented in Table 7. All mixtures meet the criteria for self-compacting concrete, primarily classified within category SF2 [38], in terms of spreadability and VS1/VF1 [38, 39] in terms of viscosity, PL2 [40] in terms of L-flowability, and SR2 [41] in terms of segregation resistance, confirming the satisfactory stability of all mixtures.

Table 7. Characterisation of fresh SCCs

	Spreadability		L-box	V-funnel	Sieve segregation	Japanese ring		16 Ø
	T_{500} (s)	mm	3 Ø	(s)	% laitance	T_{500}j	mm	PJ
SCC C	1.09	735	0.94	5.81	14	1.43	720	6
SCC S10%	1.19	725	0.92	5.62	11	1.47	714	7.5
SCC A10%	1.17	724	0.91	5.25	13	1.39	703	7
SCC W10%	1.15	715	0.93	5.47	13	1.41	705	8
SCC S15%	1.30	700	0.85	5.70	10	1.77	682	8
SCC A15%	1.26	703	0.89	5.56	10	1.72	686	7
SCC W15%	1.06	707	0.87	5.63	11	1.65	690	7.5
SCC S20%	1.39	715	0.83	5.88	9	1.90	687	7.5
SCC A20%	1.35	724	0.88	5.77	11	1.83	695	6.5
SCC W20%	1.24	730	0.86	5.71	11	1.71	701	6.5

* **Laitance** refers to a surface layer of fine particles, cement, and water

The fresh-state tests performed are shown in Figures 7 to 11: the Abrams cone spread (Figure 7), V-funnel (Figure 8), L-box (Figure 9), J-ring (Figure 10), and sieve stability (Figure 11).

Figure 7. Abrams cone spread test

Figure 8. V-funnel test

Figure 9. . L-box test

Figure 10. J-ring test

Figure 11. Sieve stability test

Figure 12 presents the slump flow diameter results for all ten SCC formulations. All mixtures recorded spread diameters ranging from 700 mm (SCC S15%) to 735 mm (CTR), placing every formulation within the SF2 class (660-750 mm), which corresponds to a medium flowability appropriate for most reinforced concrete applications without significant risk of blockage or segregation. No mixture exceeded the SF2 upper boundary, confirming that none of the calcined sediment substitutions induced excessive fluidity loss that would compromise workability.

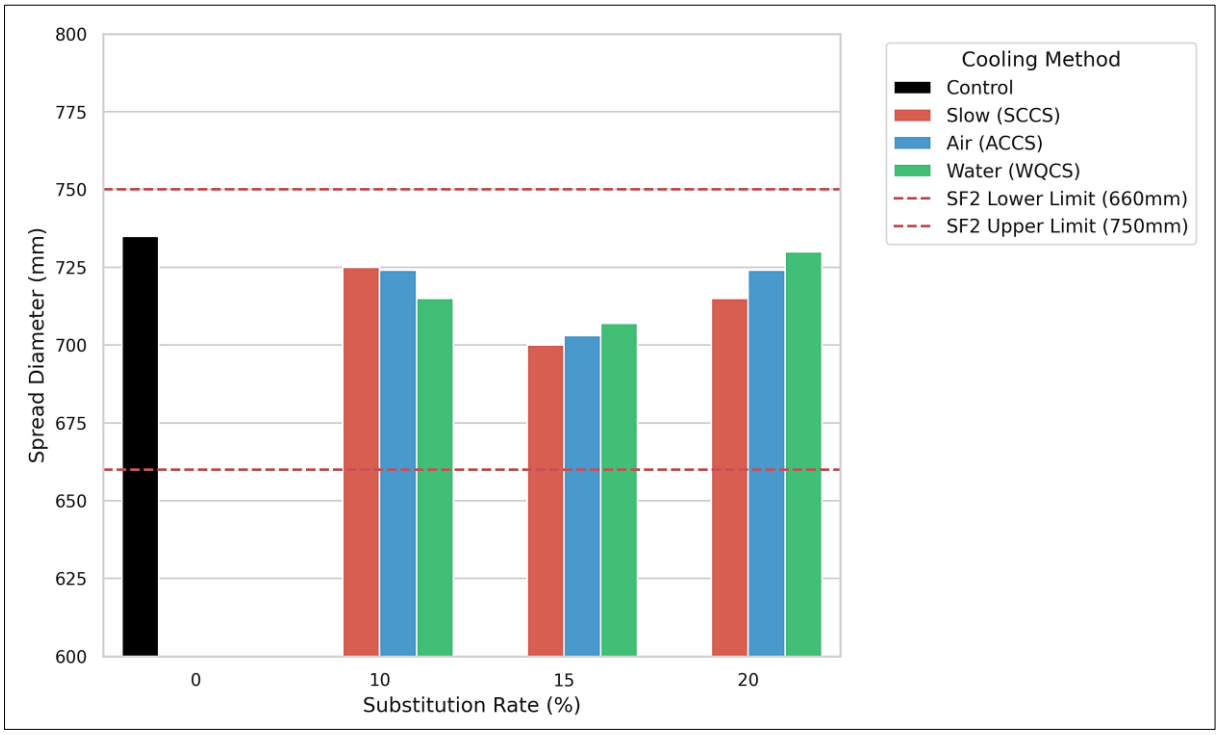

Figure 12. Slump flow test results

A clear reduction in spread diameter is observed with an increasing substitution rate, particularly for SCCS formulations: SCC S15% reaches the lower range of SF2 at 700 mm, reflecting the higher water demand and angularity associated with the partially recrystallized, less amorphous surface of slowly cooled particles. In contrast, WQCS formulations maintain significantly better fluidity at equivalent substitution rates: SCC W20% achieves 730 mm, surpassing both SCC S20% (715 mm) and SCC A20% (724 mm), a performance attributed to the smoother, more vitreous surface texture of water-quenched particles, which reduces inter-particle friction and enhances the effectiveness of superplasticiser adsorption.

T_{500} values range from 1.06 s (SCC W15%) to 1.39 s (SCC S20%), all strictly below the 2.0 s threshold defining the VS1 viscosity class, indicating that all mixtures exhibit adequate but not excessive plastic viscosity. The lowest T_{500} recorded for SCC W15% suggests that WQCS particles at moderate substitution rates may, counter-intuitively, slightly accelerate early flow due to the lower surface energy and reduced water absorption of the highly amorphous phase. Overall, the systematic compliance of all formulations with both SF2 and VS1 classifications confirms that calcined Ksob dam sediments, regardless of the cooling method can be incorporated into SCC up to 20% substitution while preserving the fundamental flow characteristics required by standard specifications.

Figure 13 illustrates the L-box filling ratios (H_2/H_1) measured with the three-bar configuration (PL2 criterion) for all formulations. All mixtures achieved ratios between 0.83 (SCC S20%) and 0.94 (CTR), uniformly satisfying the PL2 requirement of $H_2/H_1 \geq 0.80$ with three reinforcement bars, which represents the most stringent standard passing ability criterion. The use of the three-bar configuration is particularly significant: it subjects the fresh concrete to a more demanding geometric confinement than the two-bar test (PL1), making compliance with PL2 a stronger indicator of practical passability in densely reinforced structural elements.

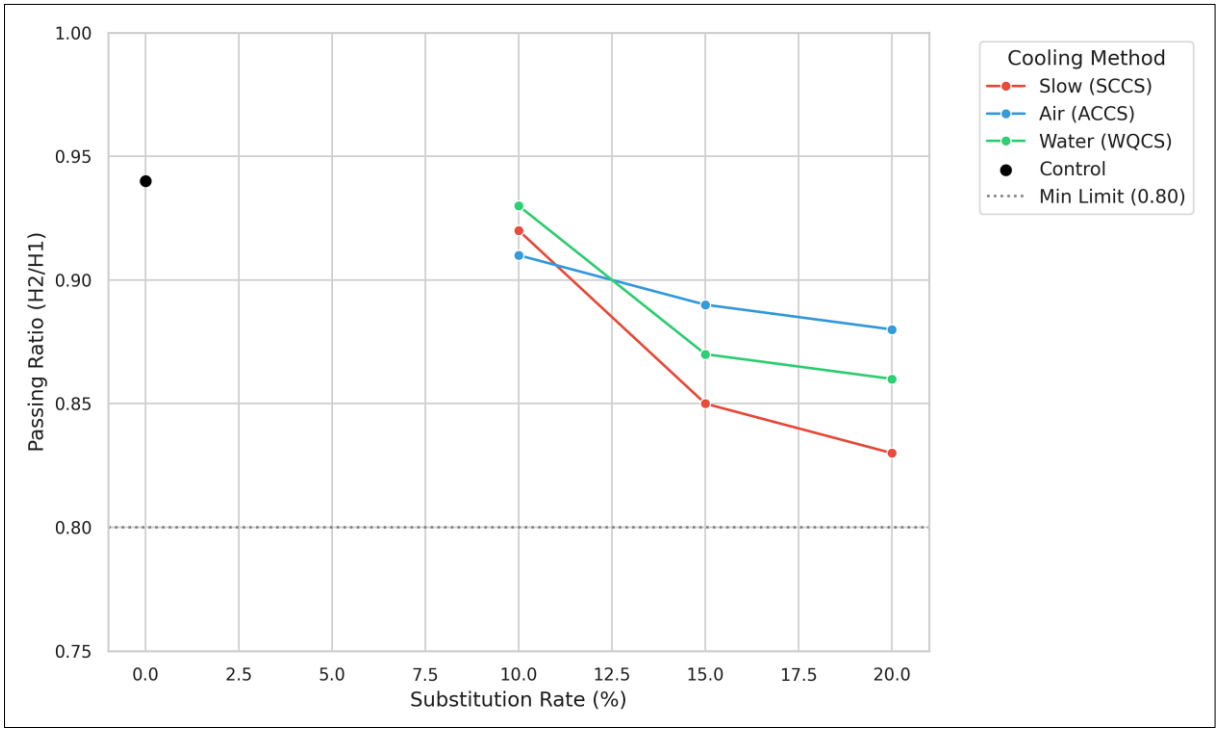

Figure 13. L-box test results (3 bars)

A progressive decrease in the H_2/H_1 ratio is observed with increasing substitution rate for all cooling methods, most pronounced for SCCS: SCC S10% records 0.92, decreasing to 0.83 at 20% substitution, approaching but never breaching the PL2 threshold. This trend reflects the combined effect of increased fine particle content, which elevates paste viscosity, and the less favourable morphology of SCCS particles that creates greater resistance to flow through the reinforcement gaps. Conversely, WQCS formulations exhibit notably higher ratios at all substitution levels: SCC W10% (0.93) is nearly equivalent to the control (0.94), and even SCC W20% (0.86) maintains a comfortable margin above the limit. This superior passability of WQCS mixtures confirms that the higher degree of amorphisation achieved through water quenching not only benefits pozzolanic reactivity but also confers rheological advantages at the fresh state, likely through improved dispersion and reduced agglomeration of fine particles.

Figure 14 shows the V-funnel flow times, which provide an indirect measure of plastic viscosity under dynamic conditions for all SCC formulations. All recorded values range from 5.25 s (SCC A10%) to 5.88 s (SCC S20%), placing every mixture well within the VF1 viscosity class (flow time < 9.0 s), and far from the VF2 upper boundary of 25.0 s. This systematic compliance confirms that none of the calcined sediment substitutions induced excessive viscosity that would impair the self-compacting behaviour under realistic casting conditions.

Notably, SCC A10% (5.25 s) exhibits a shorter flow time than the control CTR (5.81 s). This apparent improvement may be explained by a filler effect: at 10% substitution, the fine ACCS particles (BSA ≈ 13,000 cm²/g) fill the interstitial voids between cement grains, improving particle packing density and reducing internal friction without yet introducing sufficient additional surface area to significantly increase water demand. This filler-dominant regime transitions to a water-demand-dominant regime at higher substitution rates, as evidenced by the progressive increase in flow time for both ACCS and SCCS beyond 10%.

WQCS formulations showed consistently moderate flow times (5.47-5.71 s), increasing more gradually with the substitution rate than SCCS formulations (5.62-5.88 s), confirming the superior rheological efficiency of water-quenched sediments. The close correlation between V-funnel flow time trends and T_{500} trends (Figure 12) provides strong internal consistency to the viscosity characterisation, validating the rheological profile of all ten formulations across two independent test methods.

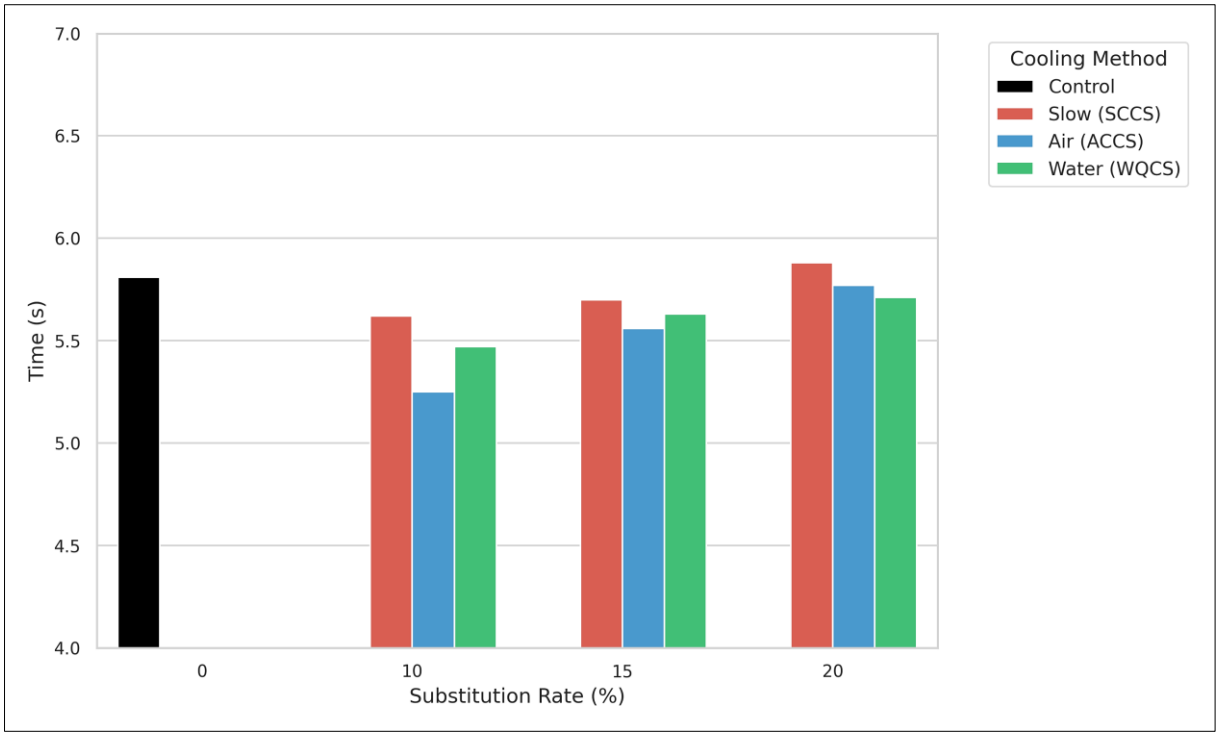

Figure 14. V-funnel flow Time results

Figure 15 presents the sieve segregation resistance (percentage of laitance) measured for all formulations. All mixtures recorded laitance percentages between 9% (SCC S20%) and 14% (CTR), all satisfying the most stringent SR2 segregation resistance class (≤ 15%), which ensures that the concrete matrix remains stable and homogeneous during and after placement. Crucially, the control concrete (CTR, 14%) sits closest to the SR2 limit, while all sediment-substituted formulations demonstrate equal or superior segregation resistance.

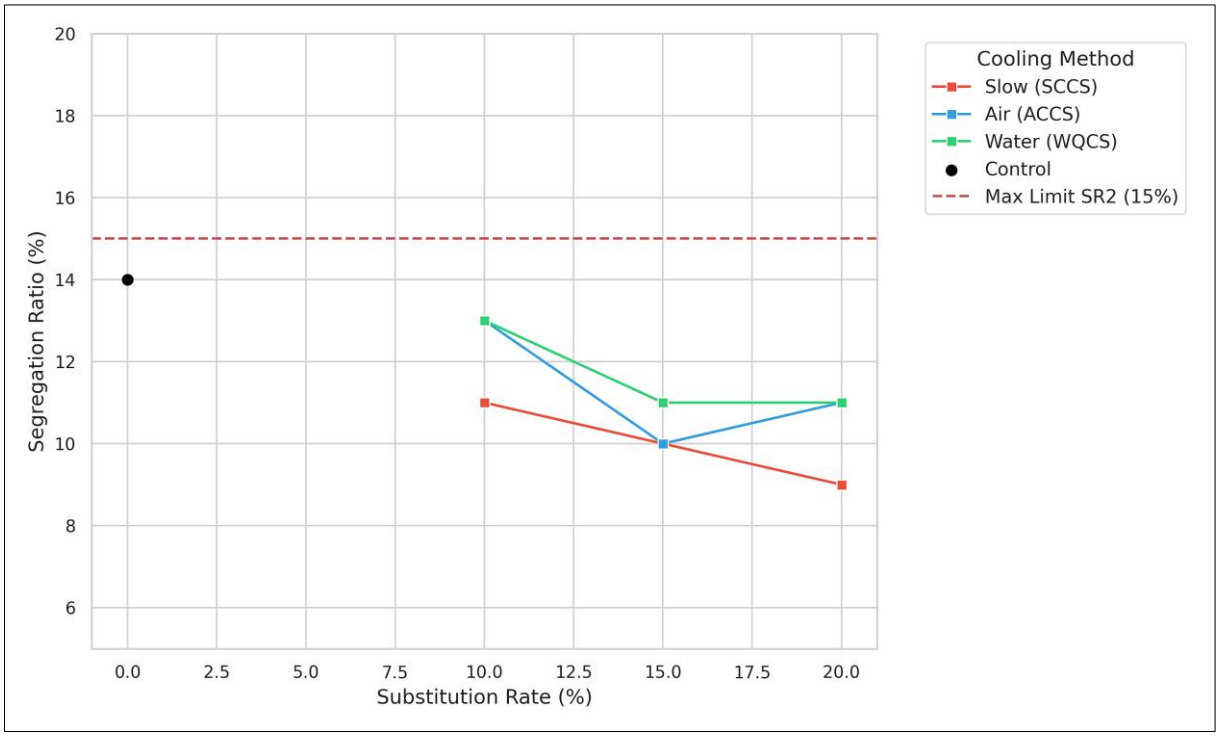

Figure 15. Sieve Segregation Resistance

A clear and systematic inverse relationship is observed between the substitution rate and segregation tendency: as the replacement level increases from 10% to 20%, the percentage of laitance decreases across all cooling methods. This counter-intuitive improvement is mechanistically explained by the high fineness of the calcined sediments (BSA ≈

13,000 cm²/g), which is approximately four times greater than that of the cement (3,129 cm²/g). The introduction of these ultra-fine particles increases the cohesiveness of the fresh paste by filling the finest pores of the granular skeleton and increasing the inter-particle contact surface, thereby reducing the tendency for free water and paste to bleed through the sieve mesh.

Among the cooling methods, SCCS formulations exhibit the lowest segregation values at all substitution rates (e.g., S20% = 9%), suggesting that the less reactive, denser surface of slowly cooled particles may exert a stronger physical containment effect on bleeding water, despite their lower pozzolanic activity. WQCS and ACCS formulations record slightly higher laitance percentages but remain well within SR2 limits. The consistent SR2 classification across all formulations confirms that the incorporation of calcined dam sediments effectively enhances the static stability of SCC, a particularly valuable property for tall structural elements where dynamic segregation is a primary concern.

Figure 16 presents the J-Ring blocking step (PJ) measured with the 16-bar configuration for all ten formulations. All PJ values lie between 6.0 mm (CTR and SCC A20%) and 8.0 mm (SCC W10%, SCC S15%, SCC W15%), all strictly satisfying the PJ2 criterion (PJ ≤ 10 mm with 16 reinforcement bars). The use of the 16-bar ring, which creates a more confined annular gap than the 12-bar configuration, makes PJ2 compliance a more rigorous indicator of flowability in the presence of closely spaced reinforcement.

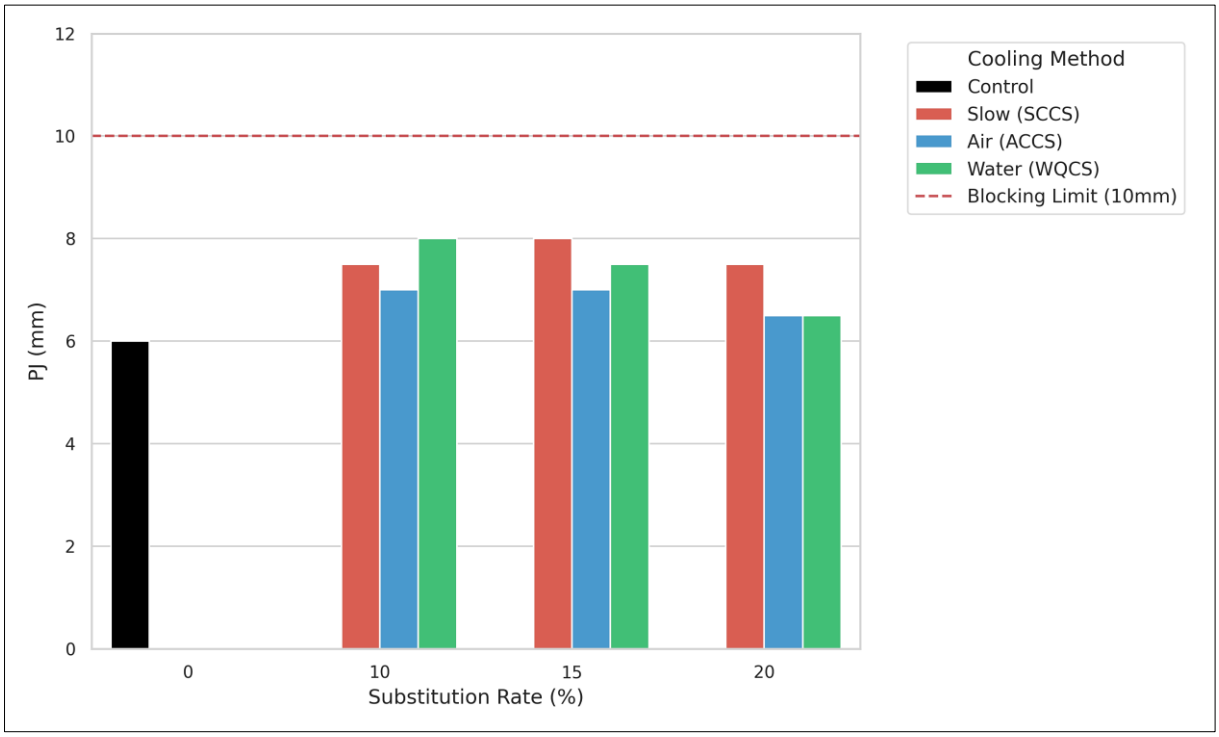

Figure 16. J-Ring test results (blocking step Pj)

The moderate increase in PJ values from CTR (6 mm) to the highest-substitution mixtures (6.5-8 mm) reflects the expected increase in paste viscosity associated with calcined sediment addition, which slightly increases the resistance to flow through the reinforcement bars. However, the fact that no formulation approaches the 10 mm limit even at 20% substitution with the most demanding cooling method demonstrates the robustness of the superplasticiser adjustment strategy adopted in this study. The consistently low PJ values across all formulations indicate that the concrete will flow around reinforcement bars with minimal differential spread, preventing the formation of aggregate-rich pockets that could compromise the homogeneity of the hardened element.

A comparison of cooling methods at equivalent substitution rates reveals that WQCS formulations tend to produce slightly higher PJ values at 10% and 15% substitution (PJ = 8 mm for W10% and W15%) than ACCS formulations, while ACCS20% records the lowest PJ (6.5 mm, equivalent to the control). This may reflect the slightly higher early-stage reactivity of ACCS particles at low substitution rates, which could locally stiffen the paste around the J-ring bars during the test window. Nonetheless, all differences remain within the PJ2 classification, and no formulation exhibits a blocking tendency, confirming universal compliance with passability requirements.

Taken together, the fresh-state characterisation results (Figures 12-16) demonstrate that all ten SCC formulations simultaneously satisfy the five standard classification criteria: SF2 for flowability, VS1/VF1 for viscosity, PL2 for passing ability, SR2 for segregation resistance, and PJ2 for J-Ring blockage. These results were achieved through a limited superplasticiser adjustment, ranging from 4.95 kg/m³ for the control to a maximum of 5.40 kg/m³ (+9.1%) for 20% substitution formulations, proved sufficient for all formulations to achieve the target performance of an SCC [42].

While a progressive reduction in fluidity is observed with the increasing substitution [26] rate most pronounced for SCCS formulations—this effect is systematically offset by the superior workability retention of WQCS mixtures, whose more amorphous particle surface enhances superplasticiser efficiency and reduces inter-particle friction. These findings establish a solid rheological foundation for the mechanical and durability investigations presented in the following sections.

3.2. Mechanical Properties

The development of compressive strength (σc) according to standard NF EN 12390-3 [43] and flexural strength (σt) according to standard NF EN 12390-5 [44] is shown in Table 8.

Table 8. Characterisation of SCCs in the hardened state (in MPa)

	7 days		14 days		28 days		90 days		180 days	
	σ_t	σ_c	σ_t	σ_c	σ_t	σ_c	σ_t	σ_c	σ_t	σ_c
CTR	7.13	57.86	8.19	61.68	9.08	72.51	9.52	79.59	**9.67**	**83.57**
S 10%	7.32	55.21	7.85	57.79	8.67	64.41	8.16	76.47	8.84	79.88
A 10%	7.81	56.26	7.96	62.46	8.14	71.05	8.29	77.40	8.98	80.06
W 10%	7.10	49.84	7.44	60.07	8.31	68.24	8.41	78.29	**9.11**	**81.17**
S 15%	7.09	41.75	6.65	50.37	7.71	60.36	8.04	71.34	8.33	74.03
A 15%	7.43	48.39	7.66	56.19	8.11	62.65	8.23	73.86	8.38	76.95
W 15%	7.11	46.87	7.74	58.80	7.49	65.04	8.28	75.35	**8.65**	**78.61**
S 20%	6.49	42.73	7.07	46.88	7.47	59.69	7.76	64.93	7.95	67.76
A 20%	6.56	41.71	7.44	48.51	7.68	61.76	7.87	68.25	**8.21**	**69.40**
W 20%	6.44	44.13	7.34	51.50	7.51	60.74	8.05	66.76	8.16	68.28

Compressive and flexural strength tests are illustrated in Figures 17 and 18, respectively.

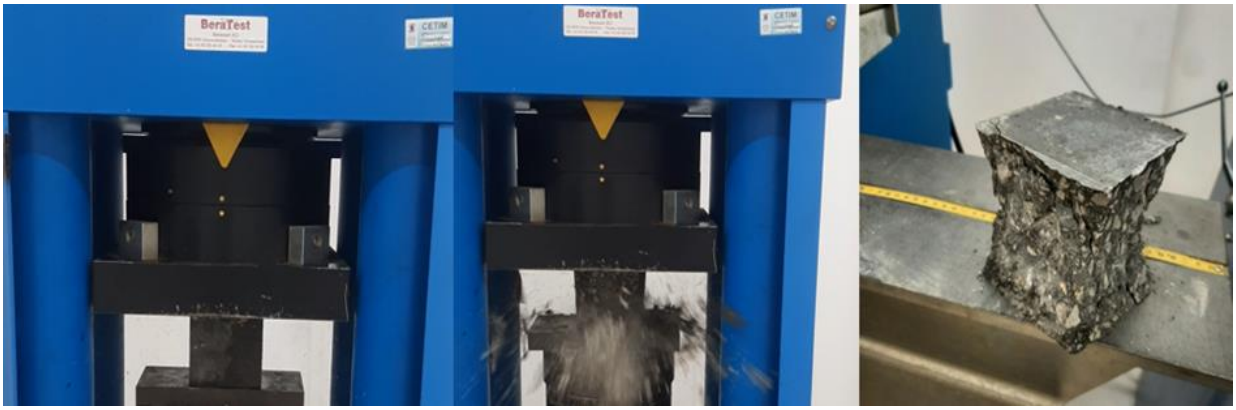

Figure 17. Compressive strength tests

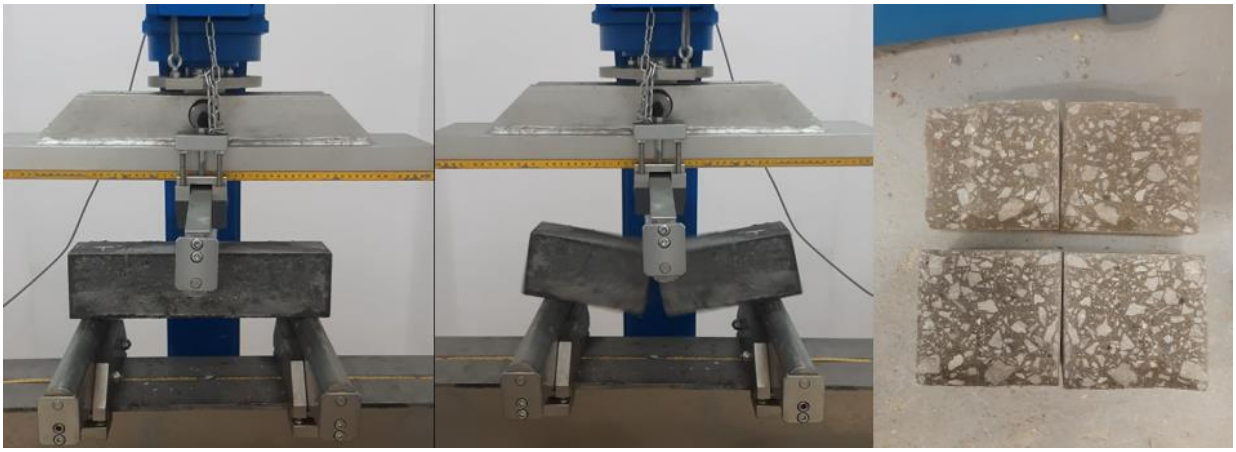

Figure 18. Flexural strength tests

Each mechanical test was performed on three replicate specimens per formulation and per age; results are reported as mean values. The coefficient of variation for compressive strength was below 3% in all cases, confirming acceptable repeatability.

Visual examination of the fractured prismatic specimens after flexural loading, illustrated in Figure 18, reveals a failure mode of significant mechanical interest. In all tested formulations, fracture occurred as a single, well-defined transverse crack perpendicular to the longitudinal axis of the prism, located at or near the mid-span loading point, consistent with the maximum bending moment distribution expected under three-point loading according to NF EN 12390-5.

The most noteworthy observation is the nature of aggregate failure at the fracture plane: limestone coarse aggregates were systematically cut cleanly through their bulk, rather than being debonded or pulled out from the surrounding cement paste. This fracture morphology; where the crack propagates transgranularly through the aggregate particles rather than circumventing them along the interfacial transition zone (ITZ); is a defining characteristic of a mature, high-quality paste–aggregate bond. In ordinary or weakly pozzolanic concrete, the ITZ typically constitutes the weakest microstructural link, and crack paths preferentially follow the paste–aggregate interface. The transgranular fracture observed here indicates that, through secondary pozzolanic C-S-H and C-A-S-H formation (particularly pronounced in WQCS formulations) the ITZ was sufficiently densified to redirect the fracture energy into the aggregate body itself, confirming that paste–aggregate bond strength exceeded the tensile strength of the limestone aggregate.

The absence of aggregate pullout or delamination across all ten formulations further confirms the structural integrity and homogeneity of the paste–aggregate interface, regardless of the cooling method applied.

The cross-sectional views of sawn prismatic specimens shown in Figure 19 provide complementary macrostructural evidence of the quality of the concrete matrix. Across all ten formulations, the cut face reveals a spatially uniform distribution of coarse and fine aggregates within the cement paste, with no visible signs of aggregate clustering, paste-rich zones, bleeding channels, or sedimentation gradients. The limestone gravels (3/8 and 8/15 fractions) are well-embedded and evenly dispersed throughout the 100 × 100 mm cross-section, and the paste appears compact and continuous between aggregate particles, with no visible macro-voids attributable to incomplete self-compaction.

Figure 19. Cross-sectional view of sawn SCC prismatic specimens (100 × 100 mm face)

This macrostructural homogeneity provides direct visual confirmation of the effectiveness of the SCC mix design and the stability of the fresh concrete during casting and curing, fully consistent with the SF2, SR2, and PJ2 classifications recorded in Table 8. In particular, the absence of any visible aggregate segregation — even at 20% sediment substitution where fine particle content is highest — demonstrates that the increased cohesion provided by the ultra-fine calcined sediments (BSA ≈ 13,000 cm²/g) successfully counteracted any tendency toward dynamic segregation during flow. The uniform paste distribution observed around each aggregate particle in all formulations, including SCCS-based concretes, further confirms that the self-compacting flow achieved complete and homogeneous filling of the mould cross-section in all cases, a prerequisite for the reliable interpretation of the mechanical and durability results presented in this study.

Figure 20 presents the progression of compressive strength (σc) for all ten SCC formulations at 7, 14, 28, 90, and 180 days of water curing.

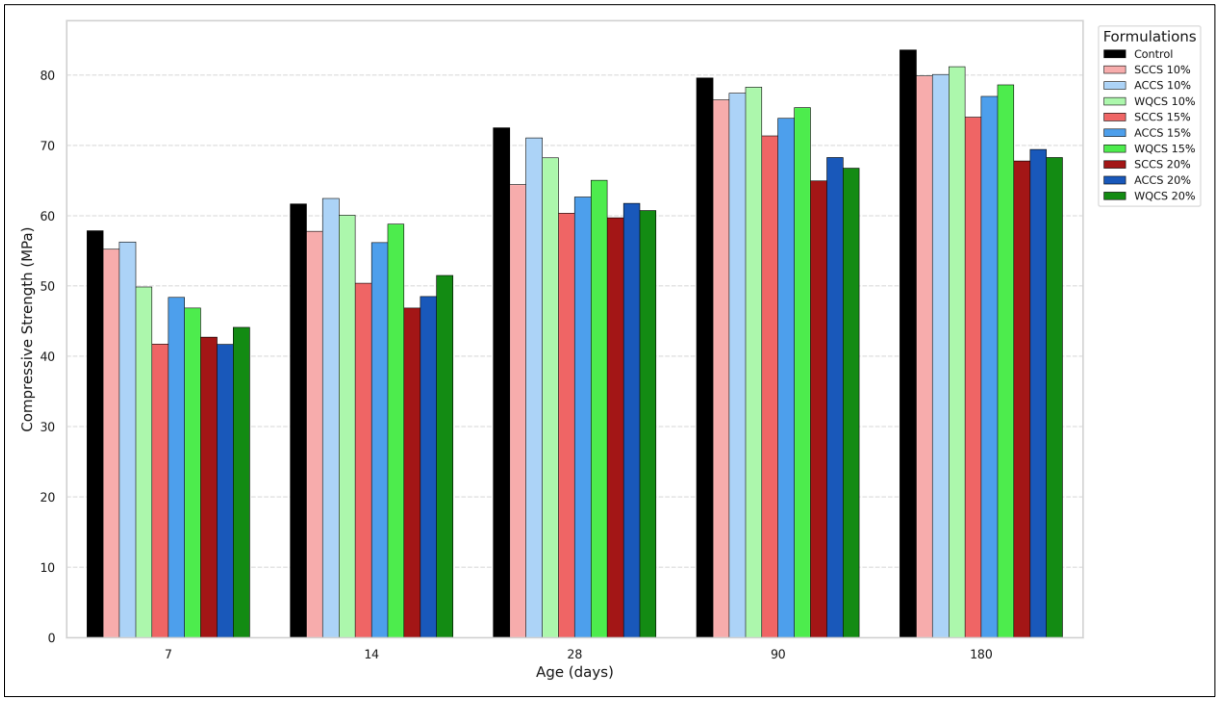

Figure 20. Compressive strength test results

Figure 21 presents the progression of flexural strength (σt) for all ten SCC formulations at 7, 14, 28, 90, and 180 days of water curing.

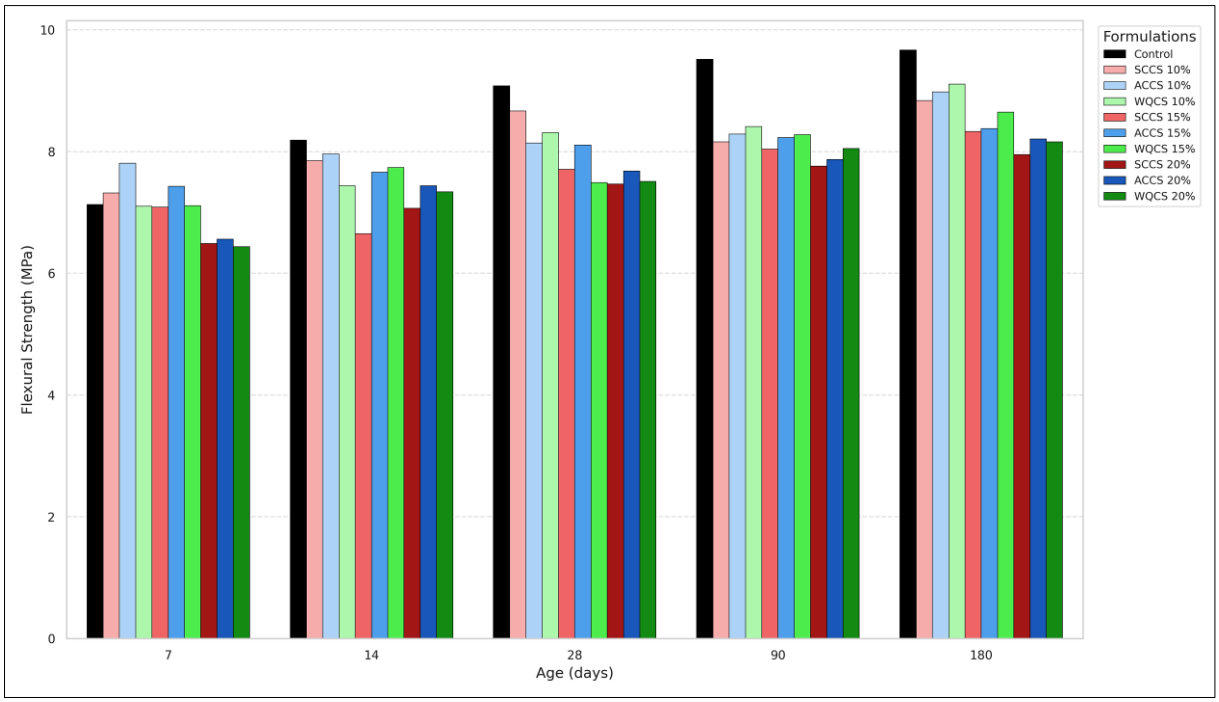

Figure 21. Flexural strength test results

Initial strengths (7 days) were generally lower than those of the control for calcined sediment-substituted concretes, reflecting the slower kinetics of the pozzolanic reaction [5, 16, 21]. However, a significant increase in strength was observed between 7 and 180 days for all modified formulations, demonstrating the medium- and long-term effectiveness of the pozzolanic reaction of dam sediments.

At 180 days, the performance of the calcined sediment-substituted concretes was similar to that of the control sample. The formulation incorporating 10% quenched calcined sediment (WQCS) achieved a compressive strength of 81.17 MPa, or 97% of the value of the control concrete (83.57 MPa). At a rate of 15%, this same formulation (WQCS15)

retained 94% of the control's strength, with a value of 78.61 MPa. Concrete with 20% substitution exhibited a more marked reduction in strength relative to the control, whilst still demonstrating a continuous increase in absolute strength over time.

Comparison of cooling methods revealed that concretes formulated with air-cooled calcined sediments (ACCS) had slightly higher strengths than other modified concretes at 7 days. However, in the longer term (90 and 180 days), it was the concretes containing water-quenched calcined sediment (WQCS) that showed the highest strengths among the modified concretes (formulations incorporating calcined sediments). Flexural tensile strengths followed similar trends to those observed for compressive strength for all formulations at all testing ages.

3.3. Thermal Analyses (TGA/DSC)

The TGA/DSC analyses carried out on the control cement pastes and those substituted with 10% and 15% of ACCS, and with 10% and 15% of WQCS confirm the pozzolanic reaction of the dam sediments used. The Differential Thermal Analysis (DTA) thermograms of the five cement pastes analysed are presented in Figures 22-a to 22-e.

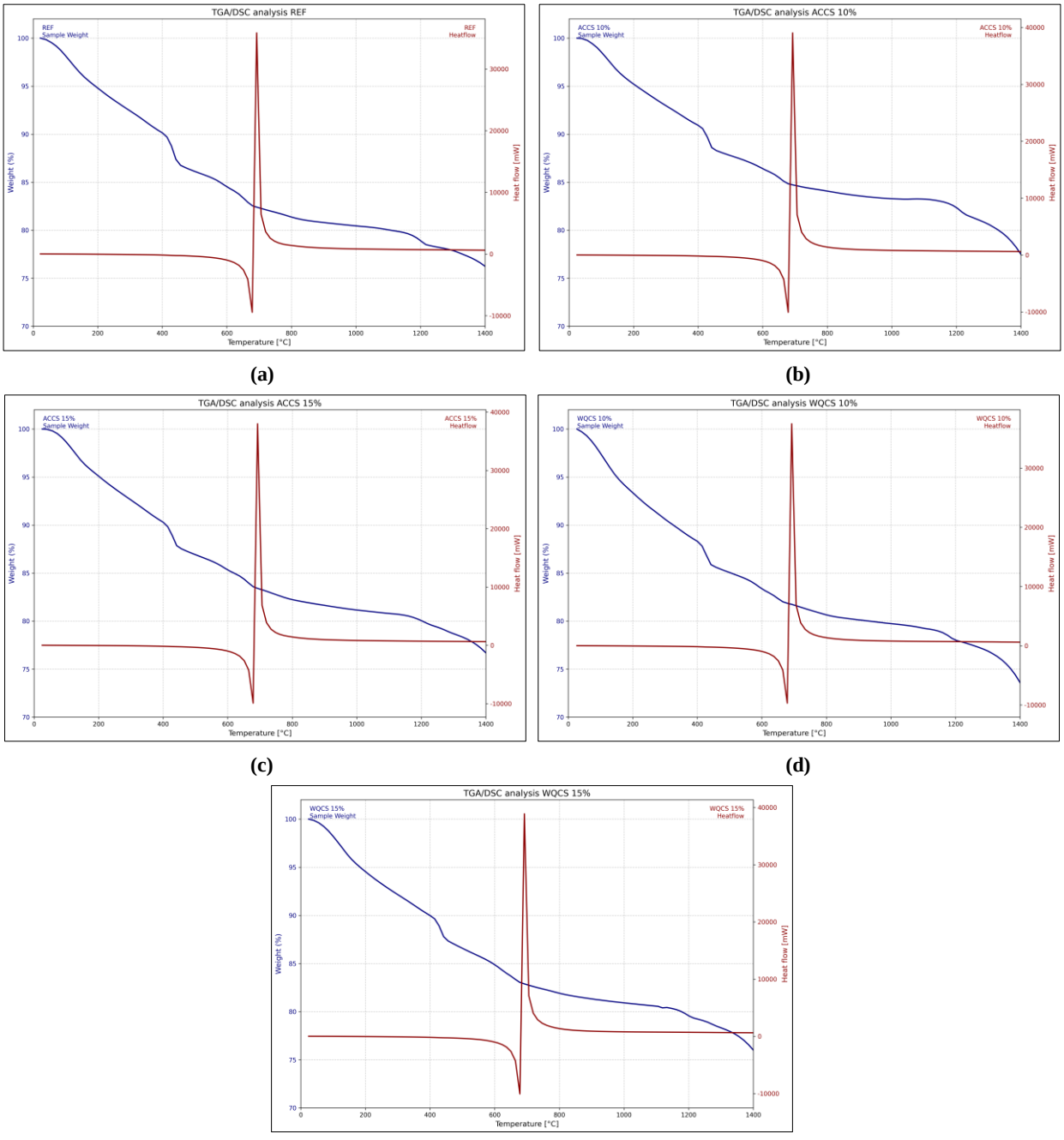

Figure 22. DTA thermograms of cement paste: (a) Control REF, (b) Contains 10% of ACCS, (c) Contains 15% of ACCS, (d) Contains 10% of WQCS, (e) Contains 15% of WQCS

The thermograms show:

1. An increased mass loss in the C-S-H dehydration zone (50-200°C) for substituted cement pastes, particularly with WQCS, indicates greater hydrate formation.
2. The portlandite ($Ca(OH)_2$) decomposition peak, around 400-500 °C, isreduced in substituted cement pastes, confirming its consumption by the pozzolanic reaction. This reduction is more pronounced for WQCS than for ACCS, and increases with the substitution rate (15% > 10%).
3. A slight increase in mass loss is observed at around 600-800°C (carbonate) for substituted cement pastes.
4. An exothermic DSC peak appears at 600-800°C, of approximately equal intensity across all samples.

These results attest to the pozzolanic reactivity of calcined sediments, which is higher for WQCS, and explain the development of long-term strength.

3.4. Durability Properties

The durability indicators measured at 180 days are presented in Table 9.

Table 9. Durability indicators for SCCs after 180 days

	Abs Imm %	Abs Boiling %	g_1 ρ Dry (g/cm³)	ρ Imm (g/cm³)	ρ Boiling (g/cm³)	g_2 ρ Apparent (g/cm³)	V_1 PPS (voids) %
CTR	4.76	5.54	1.54	1.62	1.63	1.69	8.54
S10	5.14	6.07	1.59	1.68	1.69	1.77	9.67
A10	4.51	5.36	1.56	1.63	1.64	1.70	8.37
W10	4.42	5.28	1.59	1.66	1.67	1.73	8.38
S15	5.32	6.19	1.60	1.69	1.70	1.78	9.91
A15	4.61	5.45	1.60	1.67	1.69	1.75	8.71
W15	4.66	5.49	1.59	1.67	1.68	1.74	8.73
S20	5.60	6.48	1.61	1.70	1.72	1.80	10.45
A20	4.87	5.76	1.58	1.66	1.67	1.74	9.10
W20	4.89	5.35	1.64	1.72	1.72	1.79	8.75

The durability indicators measured at 180 days, presented in Table 9, reveal distinct behaviours depending on the cooling method applied to the calcined sediments. This analysis enables an assessment of the impact of each thermal treatment on the microstructure and permeability of SCC.

Exceptional Performance of WQCS Formulations

Quantitative analysis confirms the superiority of water-quenched calcined sediments (WQCS). At 10% substitution, the W10 formulation showed a water absorption of 4.42%, a reduction of 7.1% compared with the control (4.76%). This improvement was accompanied by a permeable pore space (V_1 PPS) of 8.38%, slightly lower than the 8.54% of the control (-1.9%).

The dry bulk density (g_1) reached 1.59 g/cm³ (+3.2% vs. control), while the apparent density (g_2) rose to 1.73 g/cm³ (+2.4% vs. control), reflecting a densified microstructure due to the active pozzolanic reaction of amorphous metakaolinite [45].

Even at 20% substitution, the W20 formulation maintained remarkable performance with absorption of 4.89% (only +2.7% vs. control) and porosity of 8.75% (+2.5% vs. control), confirming the sustained effectiveness of the pozzolanic reaction of WQCS.

Intermediate performance of ACCS formulations

Air-cooled sediments (ACCS) maintained performance close to that of the control at up to 15% substitution. The A10 formulation showed an absorption of 4.51% (-5.3% lower than the control) and porosity of 8.37% (-2.0% vs. control), indicating a microstructure that remains compact.

At 15% substitution, A15 maintained an absorption of 4.61% (-3.2% vs. control) and an apparent density (g_2) of 1.75 g/cm³ (+3.6% vs. control). Beyond this threshold (20% substitution), progressive degradation was observed, with A20 showing absorption of 4.87% (+2.3% vs. control) and porosity of 9.10% (+6.6% vs. control).

Progressive Deterioration of SCCS Formulations

Slow-cooled sediments (SCCS) showed systematic deterioration in durability indicators from 10% substitution onwards. S10 showed an absorption of 5.14% (+8.0% vs control) and a porosity of 9.67% (+13.2% vs control), reflecting a less dense microstructure.

This degradation gradually increased: S15 reaches 5.32% absorption (+11.8% vs. control) and 9.91% porosity (+16.0% vs. control), while S20 peaks at 5.60% absorption (+17.6% vs. control) and 10.45% porosity (+22.4% vs. control). The apparent density (g_2) increases continuously (1.77 to 1.80 g/cm³), but this increase is accompanied by increasing open porosity, suggesting a heterogeneous microstructure with poorly filled voids.

Microstructure-durability correlation

- Cross-analysis of the parameters g_1, g_2 and V_1 PPS reveals distinct microstructural mechanisms:
- **WQCS:** The moderate increase in g_1 and g_2 is accompanied by remarkable stability in V_1 PPS, indicating homogeneous densification through the abundant formation of secondary C-S-H hydrates.
- **ACCS:** Densities increase gradually but open porosity remains controlled up to 15% substitution, reflecting moderate but effective pozzolanic reactivity.
- **SCCS:** The simultaneous increase in g_2 and V_1 PPS reflects a paradoxical microstructure: denser in mass but more permeable, characteristic of a limited pozzolanic reaction, generating less compact hydration products.

In summary, the incorporation of calcined dam sediments, particularly those cooled by water quenching, enables the maintenance or even the improvement of the durability properties of SCC, owing to the densification of the microstructure induced by the pozzolanic reaction. This valorisation thus contributes to the production of self-compacting concretes that are durable and have a low environmental impact

4. Discussion

The main objective of this study was to evaluate the influence of post-calcination cooling methods on the valorisation of Ksob dam sediments as a partial substitute for cement in self-compacting concrete (SCC). Cross-analysis of the experimental results highlights the importance of heat treatment and, above all, of cooling kinetics on the pozzolanic reactivity of sediments and, consequently, on the final properties of the concrete.

4.1. Impact of Cooling Method on Pozzolanic Reactivity

Mineralogical analysis by XRD, corroborated by the significant decrease in loss of ignition observed in the chemical analysis, confirms the effectiveness of heat treatment at 750 °C in activating raw sediments [46-48]. The major transformation observed is the dehydroxylation of kaolinite, the main clay constituent identified, into metakaolinite. This amorphous phase is known for its pozzolanic reactivity, which is essential for a positive contribution to the properties of concrete. The XRD results clearly indicate that the post-calcination cooling mode significantly modulates the degree of this transformation and the nature of the resulting phases. Water quenching (WQCS) induces further amorphisation, as evidenced by the virtual disappearance of the kaolinite peaks at 12.4°, 19.9°, 23.1°, 31.4°, 35.0°, 36.0°, 40.3°, 42.6°, 43.2°, 45.9°, 47.2°, 47.6°, 48.6°, 50.2°, 54.9°, 56.7° and 57.3° 2-theta, suggesting a highly disordered and potentially more reactive structure [49-51]. Conversely, slow cooling (SCCS) appears to allow some recrystallisation or partial preservation of the initial structure, resulting in a less reactive phase. Air cooling (ACCS) represents an intermediate state. These structural differences, induced by the cooling kinetics, are fundamental to interpreting the variable performance of concretes incorporating these different types of calcined sediments.

4.2. Formulation Optimisation

The incorporation of calcined sediments, regardless of the cooling method, significantly influences the rheological properties of SCC [42]. As expected for finely ground materials (BSA ≈ 13,000 cm²/g) used as cement substitutes , an increase in water demand was observed, resulting in a slight reduction in fluidity (decrease in spread, increase in T_{500} and V-funnel flow time) at a constant superplasticiser dosage. However, it is important to note that even with substitution rates of up to 20%, the self-compacting characteristics (slump flow/Japanese ring and L-Box for passing ability) could be maintained by reasonably adjusting the superplasticiser dosage. This confirms the technical feasibility of incorporating these sediments into SCC. Interestingly, the fineness of the sediments contributed positively to the stability of the mixtures, reducing segregation (a decrease in the percentage of laitance in the Sieve segregation test) with an increasing substitution rate. Regarding the influence of the cooling method, SCC formulated with WQCS showed better fluidity and workability compared to those with ACCS and especially SCCS, for the same substitution rate. This behaviour may be attributed to particle morphology or different physicochemical interactions at the start of hydration, favoured by the more amorphous structure of WQCS.

These findings are consistent with Ouédraogo et al. [26], who reported a progressive reduction in slump flow with increasing sediment content in SCC, and with Safhi et al. [25], who observed that dredged sediment substitution up to 20% maintained SF2 class compliance with minor superplasticiser adjustment. Similarly, Muhammad & Thienel [42] demonstrated that calcined clay-based SCCs preserved VS1/VF1 viscosity classification up to 20% replacement, in agreement with the present results. However, unlike the present study where WQCS exhibited superior rheological performance over SCCS at equal substitution rates, none of the previous studies investigated the role of the post-calcination cooling method on fresh-state properties — a gap specifically addressed here.

4.3. Development of Mechanical Properties

Analysis of mechanical strength (compression and tensile) revealed the combined impact of the substitution rate and pozzolanic reactivity induced by calcination and cooling [52, 53]. In the short term (7 days), a reduction in strength was observed with an increasing substitution rate, which is typical of pozzolanic additions, whose reaction is slower than clinker hydration [54]. However, after 28 days and more markedly in the long term (90 and 180 days), the contribution of the pozzolanic reaction became evident. SCC containing 10% calcined sediments, in particular WQCS10 and ACCS10, developed strengths very close to those of the control SCC, reaching up to 97% of the control's compressive strength at 180 days. Even at 15% substitution, the strengths obtained, particularly with WQCS15, were considered very satisfactory and compatible with many structural applications. The 20% rate led to a more noticeable decrease, although the long-term strength progression remains significant. The influence of the cooling mode on the kinetics of strength development was particularly illuminating. Whilst ACCS appeared to offer a slight short-term advantage (possibly due to a combination of the filler effect and initial reactivity), WQCS demonstrated clear superiority in the long term (90 and 180 days). This is fully consistent with the hypothesis of increased and more durable pozzolanic reactivity for water-quenched sediments, whose more amorphous structure promotes dissolution and reaction with portlandite, resulting from cement hydration.

The compressive strength of 81.17 MPa achieved by W10% at 180 days (97% of the control) is notably superior to the ~65 MPa reported at 360 days by Safer et al. [17] for Chorfa dam SCC. Rozière et al. [21] reported that 20% dredged sediment substitution in SCC maintained compressive strength close to the control at 90 days, a result partially corroborated in the present study by WQCS formulations but not by SCCS, underlining the critical additional influence of the cooling method. Compared to metakaolin-based SCC literature, where 10–15% MK replacement typically yields strength increases of 5–15% over the control at 28 days, the present calcined sediment formulations show lower short-term performance but competitive long-term values, reflecting the slower pozzolanic kinetics of dam sediments relative to industrially processed metakaolin.

4.4. Correlation with Thermal Analysis (TGA/DSC)

The results of the TGA/DSC thermal analysis corroborate and explain the observations made on mechanical strength. The analysis focused on the most effective formulations (CTR, ACCS10, ACCS15, WQCS10, WQCS15). The greater mass loss in the C-S-H dehydration range (50-200°C) and the increased intensity of the corresponding endothermic peak in DSC for the substituted samples [25], especially WQCS10 and WQCS15, directly indicate increased production of binding hydrates. At the same time, the significant reduction in the amount of residual portlandite (decomposition peak around 400-500 °C), particularly marked for WQCS10, attests to the consumption of $Ca(OH)_2$ by the pozzolanic reaction. Comparison between ACCS and WQCS cement paste samples confirms the superior reactivity of water-quenched sediments (WQCS). The greater quantity of hydrates formed and the more efficient consumption of portlandite (a potentially less stable hydration product and source of weakness) directly explain the better long-term mechanical performance and denser microstructure observed for WQCS-based concretes.

4.5. Durability and Practical Applications

Durability tests, according to ASTM C642-13 [37], carried out at 180 days, confirmed the beneficial impact of an effective pozzolanic reaction on the microstructure and permeability of concrete [55]. Whilst the addition of fines may increase initial porosity, the pozzolanic reaction (by generating additional C-S-H) tends to refine the porous structure and reduce pore connectivity [56]. The results of water absorption (immersion and boiling) and water-accessible porosity (WAP) showed that while slow cooling (SCCS) leads to increased porosity compared with the control, air cooling (ACCS) mitigates this effect, and water cooling (WQCS) produces concrete with porosity and absorption comparable to or even lower than that of the control concrete, even for substitution rates of 20%. This more closed microstructure, particularly obtained with WQCS, is a key indicator of better potential durability, as it limits the penetration of aggressive agents (water, chlorides, sulphates, and CO_2) responsible for the degradation of concrete in service [57].

The beneficial microstructural densification observed here for WQCS formulations corroborates the findings of Paiva et al. [45] and Ibrahim et al. [56], who demonstrated that efficient pozzolanic C-S-H formation reduces pore connectivity and water absorption in pozzolan-containing concrete.

4.6. Industrial Feasibility of Post-Calcination Cooling Methods

Among the three cooling protocols investigated, air cooling (ACCS) presents the highest immediate industrial feasibility. Its integration into existing rotary or tunnel kiln production lines requires no additional infrastructure, as the calcined material simply cools on a discharge conveyor in ambient air — a process already standard in metakaolin and calcined lime industries [58]. In contrast, slow furnace cooling (SCCS) reduces kiln throughput significantly due to its 24-hour cooling cycle, making it economically unviable at large scale despite its technical simplicity. Water quenching (WQCS), while delivering the best pozzolanic and mechanical performance, requires dedicated engineering development before it can be applied industrially. Adapting continuous rapid-cooling systems (such as spray cooling or drum quenching with closed-loop water recycling) to large-scale sediment calcination represents a significant engineering challenge for cement industry engineers, with the dual objective of maximising pozzolanic reactivity while minimising water consumption and environmental impact. Air cooling is therefore recommended as the most viable near-term industrial solution, while water quenching remains a high-priority development target for optimised eco-efficient SCC production.

5. Conclusion

This study provides the first systematic investigation of the influence of post-calcination cooling kinetics on the pozzolanic performance of Ksob dam sediments (Algeria) as partial cement substitutes in self-compacting concrete (SCC). Three cooling protocols (water quenching (WQCS), air cooling (ACCS), and slow furnace cooling (SCCS)) were applied following calcination at 750 °C for 5 hours across mineralogical, rheological, mechanical, and durability dimensions on ten SCC formulations at substitution rates of 10%, 15%, and 20%.

XRD analysis confirmed that calcination successfully converted kaolinite into amorphous metakaolinite; however, the degree of amorphisation was critically governed by cooling rate. Water quenching preserved the highest structural disorder by suppressing recrystallisation, evidenced by the near-complete disappearance of kaolinite diffraction peaks, while slow furnace cooling allowed partial structural reorganisation, reducing pozzolanic potential. Air cooling produced intermediate behaviour.

In the fresh state, all ten formulations satisfied the five normative SCC criteria: SF2 for flowability and filling capacity; VS1/VF1 for flow time and viscosity; PL2 for filling ability and resistance to blocking; SR2 for resistance to static segregation; and PJ2 for passing ability. These results were achieved through iterative mix optimisation, requiring only a modest superplasticiser adjustment from 1.10% to 1.20% of binder mass.

In the hardened state, WQCS formulations exhibited superior long-term performance: W10% reached 81.17 MPa at 180 days (97% of the control at 83.57 MPa), while W15% retained 94% at 78.61 MPa. TGA/DSC analyses confirmed these gains are attributable to enhanced secondary C-S-H formation and accelerated portlandite consumption. Long-term durability further confirmed this superiority: W10% showed 7.1% lower water absorption and 1.9% lower permeable porosity than the control. Conversely, SCCS formulations showed systematic deterioration, reaching +17.6% water absorption and +22.4% permeable porosity at 20% substitution.

From an industrial perspective, air cooling represents the most viable near-term solution given compatibility with existing calcination infrastructure. Water quenching, while technically superior, requires dedicated engineering development of continuous closed-loop rapid-cooling systems. Future research should address long-term durability under aggressive exposure conditions (chloride, sulphate, carbonation), ternary binder systems combining WQCS with limestone filler, and the development of a regulatory framework for calcined sediment-based SCMs, for which the 20% substitution threshold represents a scientifically grounded reference point

6. Nomenclature

Abbreviation	Definition	Abbreviation	Definition
SCC	Self-Compacting Concrete	**Sx %**	SCC S with (x % Cement + y % SCCS)
US	Uncalcined Sediment	**Ax %**	SCC A with (x % Cement + y % ACCS)
WQCS	Water-Quenched Calcined Sediment	**Wx %**	SCC W with (x % Cement + y % WQCS)
SCCS	Slow-Cooled Calcined Sediment (furnace)	**SCMs**	Supplementary Cementitious Materials
CTR	Control formulation (100% cement)	**BSA**	Blaine Specific Area

7. Declarations

7.1. Author Contributions

Conceptualization, A.S., R.C., and E.-H.K.; methodology, A.S. and R.C.; validation, A.S., R.C., and E.-H.K..; formal analysis, A.S.; investigation, A.S.; resources, A.S. and R.C.; data curation, A.S.; writing—original draft preparation, A.S.; writing—review and editing, A.S., R.C., and E.-H.K.; visualization, A.S.; supervision, R.C. and E.-H.K.; project administration, A.S.; funding acquisition, A.S. and R.C. All authors have read and agreed to the published version of the manuscript.

7.2. Data Availability Statement

The data presented in this study are available in the article.

7.3. Funding

The authors received no financial support for the research, authorship, and/or publication of this article.

7.4. Conflicts of Interest

The authors declare no conflict of interest.

8. References

[1] Minocha, S., & Hossain, F. (2025). GRILSS: opening the gateway to global reservoir sedimentation data curation. Earth System Science Data, 17(4), 1743–1759. doi:10.5194/essd-17-1743-2025.

[2] Lee, F. Z., Lai, J. S., & Sumi, T. (2022). Reservoir Sediment Management and Downstream River Impacts for Sustainable Water Resources—Case Study of Shihmen Reservoir. Water (Switzerland), 14(3), 479. doi:10.3390/w14030479.

[3] Castro, P. W., & Mantilla, C. A. (2021). Implementation of Strategies for the Management of Dams with Sedimented Reservoirs. Water Resources Management, 35(13), 4399–4413. doi:10.1007/s11269-021-02956-7.

[4] Rakshith, S., & Singh, D. N. (2017). Utilization of Dredged Sediments: Contemporary Issues. Journal of Waterway, Port, Coastal, and Ocean Engineering, 143(3), 4016025. doi:10.1061/(asce)ww.1943-5460.0000376.

[5] Yoobanpot, N., Jamsawang, P., Simarat, P., Jongpradist, P., & Likitlersuang, S. (2020). Sustainable reuse of dredged sediments as pavement materials by cement and fly ash stabilization. Journal of Soils and Sediments, 20(10), 3807–3823. doi:10.1007/s11368-020-02635-x.

[6] Abidi, I., Benamara, L., Correia, A. A. S., Pinto, M. I. M., & Cunha, P. P. (2021). Characterization of dredged sediments of Bouhanifia dam: potential use as a raw material. Arabian Journal of Geosciences, 14(23), 2631. doi:10.1007/s12517-021-08742-4.

[7] Solanki, P., Jain, B., Hu, X., & Sancheti, G. (2023). A Review of Beneficial Use and Management of Dredged Material. In Waste, 1(3). 815–840. doi:10.3390/waste1030048.

[8] Martellotta, A. M. N., & Levacher, D. (2025). Contaminant Assessment and Potential Ecological Risk Evaluation of Lake Shore Surface Sediments. Water (Switzerland), 17(14), 2042. doi:10.3390/w17142042.

[9] Benhaddou, K., Souileh, A., Mabrouk, A., Ouadif, L., Abdelhak, S., Baba, K., & Rharouss, M. (2025). Sustainable valorization of marine dredged sediments from Jebha Port as a partial sand replacement in eco-friendly concrete. Journal of Ecological Engineering, 26(6), 120–133. doi:10.12911/22998993/202133.

[10] Fořt, J., Afolayan, A., Kočí, V., Scheinherrová, L., Jan, J., Borovec, J., & Černý, R. (2025). Potential of water sediments in construction materials: Current approaches and critical consideration of future challenges. Heliyon, 11(1), e41121. doi:10.1016/j.heliyon.2024.e41121.

[11] Shah, I. H., Miller, S. A., Jiang, D., & Myers, R. J. (2022). Cement substitution with secondary materials can reduce annual global CO2 emissions by up to 1.3 gigatons. Nature Communications, 13(1), 5758. doi:10.1038/s41467-022-33289-7.

[12] Mejía De Gutiérrez, R., Torres, J., Vizcayno, C., & Castello, R. (2008). Influence of the calcination temperature of kaolin on the mechanical properties of mortars and concretes containing metakaolin. Clay Minerals, 43(2), 177–183. doi:10.1180/claymin.2008.043.2.02.

[13] Erasmus, E. (2016). The effect of heat treatment on the properties of kaolin. Hemijska Industrija, 70(5), 595–601. doi:10.2298/HEMIND150720066E.

[14] Kang, S. H., Kwon, Y. H., & Moon, J. (2022). Influence of calcination temperature of impure kaolinitic clay on hydration and strength development of ultra-high-performance cementitious composite. Construction and Building Materials, 326, 126920. doi:10.1016/j.conbuildmat.2022.126920.

[15] Zunino, F., & Scrivener, K. (2024). Reactivity of kaolinitic clays calcined in the 650 °C–1050 °C temperature range: Towards a robust assessment of overcalcination. Cement and Concrete Composites, 146, 105380. doi:10.1016/j.cemconcomp.2023.105380.

[16] Du, H., & Pang, S. D. (2018). Value-added utilization of marine clay as cement replacement for sustainable concrete production. Journal of Cleaner Production, 198, 867–873. doi:10.1016/j.jclepro.2018.07.068.

[17] Safer, O., Belas, N., Belaribi, O., Belguesmia, K., Bouhamou, N. E., & Mebrouki, A. (2018). Valorization of Dredged Sediments as a Component of Vibrated Concrete: Durability of These Concretes against Sulfuric Acid Attack. International Journal of Concrete Structures and Materials, 12(1), 44. doi:10.1186/s40069-018-0270-7.

[18] Akhnoukh, A., Nelson, L., & Campbell, M. (2024). Recycled Dredged Sediments as a Supplementary Cementitious Materials in Concrete Production. Proceedings of 60th Annual Associated Schools, 5, 804–794. doi:10.29007/k9mz.

[19] Safer, O., Amer, A. A. M., Belaribi, O., Belguesmia, K., Belas, N., Chemmam, M., Nougar, B., Menad, K., Chaib, O., & M'hamed, A. (2024). Study of the impact of sediments on the mechanical behavior of concrete and towards the penetration of carbon dioxide. Studies in Engineering and Exact Sciences, 5(1), 3022–3055. doi:10.54021/seesv5n1-151.

[20] Mouanda, G. F. M., Abuodha, S. O., & Thuo, J. N. (2022). Gum Arabic as an Admixture in Modified Concrete Mixed with Calcined Kaolin. Civil Engineering Journal (Iran), 8(5), 985–998. doi:10.28991/CEJ-2022-08-05-010.

[21] Rozière, E., Samara, M., Loukili, A., & Damidot, D. (2015). Valorisation of sediments in self-consolidating concrete: Mix-design and microstructure. Construction and Building Materials, 81, 1–10. doi:10.1016/j.conbuildmat.2015.01.080.

[22] Okamura, H., & Ouchi, M. (2003). Self-compacting concrete. Journal of Advanced Concrete Technology, 1(1), 5-15. doi:10.3151/jact.1.5.

[23] Mathews, M. E., Kiran, T., Nammalvar, A., Anbarasu, M., Kanagaraj, B., & Andrushia, D. (2023). Evaluation of the Rheological and Durability Performance of Sustainable Self-Compacting Concrete. Sustainability (Switzerland), 15(5), 4212. doi:10.3390/su15054212.

[24] Sallai, H. H., Bouhamou, N. E., Marouf, H., Belghit, A., & Aydin, A. C. (2024). Influence of calcined dam mud on the thermal conductivity of binary and ternary self-compacting concrete mixtures using the equivalent mortar method. Studies in Engineering and Exact Sciences, 5(1), 501–524. doi:10.54021/seesv5n1-029.

[25] Safhi, A. el M., Rivard, P., Yahia, A., Benzerzour, M., & Khayat, K. H. (2020). Valorization of dredged sediments in self-consolidating concrete: Fresh, hardened, and microstructural properties. Journal of Cleaner Production, 263, 121472. doi:10.1016/j.jclepro.2020.121472.

[26] Ouédraogo, N. P., Becquart, F., Benzerzour, M., & Abriak, N. E. (2021). Influence of fine sediments on rheology properties of self-compacting concretes. Powder Technology, 392, 544–557. doi:10.1016/j.powtec.2021.07.035.

[27] Rizal, N. S., Arifi, E., & Mufarida, N. A. (2025). High Initial Concrete Compressive Strength with Variations of Superplasticizer and Silica Fume Additions. Civil Engineering Journal, 11(1), 107–119. doi:10.28991/CEJ-2025-011-01-07.

[28] NF EN 197-1. (2012). Cement - Part 1: Composition, specifications and conformity criteria for common cements. Association Française de Normalisation (AFNOR), La Plaine Saint-Denis, France.

[29] NF EN 12620+A1. (2008) AFNOR, Aggregates for concrete. Association Française de Normalisation (AFNOR), La Plaine Saint-Denis, France.

[30] NF EN 934-2+A1. (2012). Admixtures for concrete, mortar and grout - Part 2: concrete admixtures - Definitions, requirements, conformity, marking and labelling. Association Française de Normalisation (AFNOR), La Plaine Saint-Denis, France.

[31] Vizcaíno Andrés, L. M., Antoni, M. G., Alujas Diaz, A., Martirena Hernández, J. F., & Scrivener, K. L. (2015). Effect of fineness in clinker-calcined clays-limestone cements. Advances in Cement Research, 27(9), 546–556. doi:10.1680/jadcr.14.00095.

[32] NF EN 196-2. (2013). Methods of Testing Cement - Part 2: Chemical Analysis of Cement. Association Française de Normalisation (AFNOR), La Plaine Saint-Denis, France.

[33] NF EN 196-6. (2018). Methods of testing cement - Determination of fineness. Association Française de Normalisation (AFNOR), La Plaine Saint-Denis, France.

[34] NF EN 196-1. (2016). Methods of testing cement - Part 1: Determination of strength. Association Française de Normalisation (AFNOR), La Plaine Saint-Denis, France.

[35] NF EN 933-1. (2012). Tests for geometrical properties of aggregates - Part 1: Determination of particle size distribution - Sieving method. Association Française de Normalisation (AFNOR), La Plaine Saint-Denis, France.

[36] NF EN 206+A2/CN. (2022). Concrete - Specification, performance, production and conformity - National addition to the standard NF EN 206+A2. Association Française de Normalisation (AFNOR), La Plaine Saint-Denis, France.

[37] ASTM C642-13. (2022). Standard Test Method for Density, Absorption, and Voids in Hardened Concrete. ASTM International, Pennsylvania, United States. doi:10.1520/C0642-13.

[38] NF EN 12350-8. (2019). Testing fresh concrete - Part 8: self-compacting concrete - Slump-flow test. Association Française de Normalisation (AFNOR), La Plaine Saint-Denis, France.

[39] NF EN 12350-9. (2010). Testing fresh concrete - Part 9: self-compacting concrete - V-funnel test. Association Française de Normalisation (AFNOR), La Plaine Saint-Denis, France.

[40] NF EN 12350-10, Testing fresh concrete - Part 10: self-compacting concrete - L-box test. Association Française de Normalisation (AFNOR), La Plaine Saint-Denis, France.

[41] NF EN 12350-11. (2010). Testing fresh concrete - Part 11: self-compacting concrete - Sieve segregation test. Association Française de Normalisation (AFNOR), La Plaine Saint-Denis, France.

[42] Muhammad, A., & Thienel, K. C. (2023). Properties of Self-Compacting Concrete Produced with Optimized Volumes of Calcined Clay and Rice Husk Ash—Emphasis on Rheology, Flowability Retention and Durability. Materials, 16(16), 5513. doi:10.3390/ma16165513.

[43] NF EN 12390-3. (2019). Testing hardened concrete - Part 3: Compressive strength of test specimens. Association Française de Normalisation (AFNOR), La Plaine Saint-Denis, France.

[44] NF EN 12390-5. (2019). Testing hardened concrete - Part 5: flexural strength of test specimens. Association Française de Normalisation (AFNOR), La Plaine Saint-Denis, France.

[45] Paiva, H., Silva, A. S., Velosa, A., Cachim, P., & Ferreira, V. M. (2017). Microstructure and hardened state properties on pozzolan-containing concrete. Construction and Building Materials, 140, 374–384. doi:10.1016/j.conbuildmat.2017.02.120.

[46] Benzerzour, M., Maherzi, W., Amar, M. A. A., Abriak, N. E., & Damidot, D. (2018). Formulation of mortars based on thermally treated sediments. Journal of Material Cycles and Waste Management, 20(1), 592–603. doi:10.1007/s10163-017-0626-0.

[47] Hadj Sadok, R., Belas, N., Tahlaiti, M., & Mazouzi, R. (2021). Reusing calcined sediments from Chorfa II dam as partial replacement of cement for sustainable mortar production. Journal of Building Engineering, 40, 102273. doi:10.1016/j.jobe.2021.102273.

[48] AMAR, M., Benzerzour, M., & Abriak, N. (2022). Designing Efficient Flash-Calcined Sediment-Based Ecobinders. SSRN Electronic Journal, 15(20), 7107. doi:10.2139/ssrn.4161378.

[49] Ferone, C., Liguori, B., Capasso, I., Colangelo, F., Cioffi, R., Cappelletto, E., & Di Maggio, R. (2015). Thermally treated clay sediments as geopolymer source material. Applied Clay Science, 107, 195–204. doi:10.1016/j.clay.2015.01.027.

[50] Zunino, F., Boehm-Courjault, E., & Scrivener, K. (2020). The impact of calcite impurities in clays containing kaolinite on their reactivity in cement after calcination. Materials and Structures/Materiaux et Constructions, 53(2), 1–15. doi:10.1617/s11527-020-01478-9.

[51] Sánchez, I., de Soto, I. S., Casas, M., Vigil de la Villa, R., & García-Giménez, R. (2020). Evolution of Metakaolin Thermal and Chemical Activation from Natural Kaolin. Minerals, 10(6), 534. doi:10.3390/min10060534.

[52] Snellings, R., Cizer, Ö., Horckmans, L., Durdziński, P. T., Dierckx, P., Nielsen, P., Van Balen, K., & Vandewalle, L. (2016). Properties and pozzolanic reactivity of flash calcined dredging sediments. Applied Clay Science, 129, 35–39. doi:10.1016/j.clay.2016.04.019.

[53] Hollanders, S., Adriaens, R., Skibsted, J., Cizer, Ö., & Elsen, J. (2016). Pozzolanic reactivity of pure calcined clays. Applied Clay Science, 132–133, 552–560. doi:10.1016/j.clay.2016.08.003.

[54] Chu, D. C., Amar, M., Kleib, J., Benzerzour, M., Betrancourt, D., Abriak, N. E., & Nadah, J. (2022). The Pozzolanic Activity of Sediments Treated by the Flash Calcination Method. Waste and Biomass Valorization, 13(12), 4963–4982. doi:10.1007/s12649-022-01789-8.

[55] Setina, J., Gabrene, A., & Juhnevica, I. (2013). Effect of pozzolanic additives on structure and chemical durability of concrete. Procedia Engineering, 57, 1005–1012. doi:10.1016/j.proeng.2013.04.127.

[56] Ibrahim, M., Johari, M. A. M., Hussaini, S. R., Rahman, M. K., & Maslehuddin, M. (2020). Influence of pore structure on the properties of green concrete derived from natural pozzolan and nanosilica. Journal of Sustainable Cement-Based Materials, 9(4), 233–257. doi:10.1080/21650373.2020.1715901.

[57] Safhi, A. el M., Rivard, P., Yahia, A., Henri Khayat, K., & Abriak, N. E. (2021). Durability and transport properties of SCC incorporating dredged sediments. Construction and Building Materials, 288, 123116. doi:10.1016/j.conbuildmat.2021.123116.

[58] San Nicolas, R., Cyr, M., & Escadeillas, G. (2013). Characteristics and applications of flash metakaolins. Applied Clay Science, 83–84, 253–262. doi:10.1016/j.clay.2013.08.036.